

CHARACTERIZATION OF MECHANICAL PROPERTIES IN HYBRIDIZED
FLAX AND CARBON FIBER COMPOSITES

A Thesis
Submitted to the Graduate Faculty
of the
North Dakota State University
of Agriculture and Applied Science

By

Jeffrey Michael Flynn

In Partial Fulfillment of the Requirements
for the Degree of
MASTER OF SCIENCE

Major Program:
Mechanical Engineering

May 2013

Fargo, North Dakota

North Dakota State University
Graduate School

Title

Characterization of mechanical properties in hybridized flax and carbon fiber
composites

By

Jeffrey Michael Flynn

The Supervisory Committee certifies that this *disquisition* complies with North Dakota State
University's regulations and meets the accepted standards for the degree of

MASTER OF SCIENCE

SUPERVISORY COMMITTEE:

Dr. Chad Ulven

Chair

Dr. Erik Hobbie

Dr. Long Jiang

Dr. Bora Suzen

Approved:

May 10, 2013

Date

Dr. Alan Kallmeyer

Department Chair

ABSTRACT

Natural fiber composites have been found to exhibit suitable mechanical properties for general applications. However, when high strength applications are required, natural fibers are typically not considered as a practical fiber. One method for increasing the field of application for natural fibers is by increasing their mechanical properties through hybridizing them with synthetic fibers. The effects of hybridizing flax fibers with carbon fibers were investigated in this research to determine the trends in mechanical properties resulting from varied carbon and flax fiber volumes. The research found an increase in mechanical properties when compared to 6061 aluminum at matching composite stiffness values. The following mechanical property gains were obtained: 2% tensile chord modulus, 252% tensile strength, 114% damping ratio, and a 49% weight savings. Experimental tensile values were also compared to tradition modulus prediction models such as rule of mixtures and Halpin-Tsai, and were found to be in good agreement.

TABLE OF CONTENTS

ABSTRACT.....	iii
LIST OF TABLES	vii
LIST OF FIGURES	viii
1. INTRODUCTION	1
1.1. Overview of Hybridized Composites.....	1
1.2. Natural Fibers.....	3
1.3. Carbon Fibers.....	8
1.4. Vacuum Assisted Resin Transfer Molding	12
1.5. Modeling Theory.....	13
<i>1.5.1. Rule of mixtures model</i>	<i>15</i>
1.5.1.1. Derivation	15
1.5.1.2. Factors effecting actual composite properties.....	17
1.5.1.3. Fiber misalignment	17
1.5.1.4. Discontinuous fibers	18
1.5.1.5. Interfacial bonding.....	18
1.5.1.6. Residual stresses	20
<i>1.5.2. Halpin-Tsai model</i>	<i>20</i>
<i>1.5.3. Rule of hybrid mixtures.....</i>	<i>22</i>

2. OBJECTIVES OF RESEARCH.....	26
3. MATERIALS AND METHODS.....	28
3.1. Carbon Fiber.....	28
3.2. Flax Fiber	28
3.3. Epoxy Resin	29
3.3. Materials Processing	29
3.4. Flexure Tests	33
3.5. Tensile Tests.....	33
3.6. Impact Tests	34
3.7. Vibration Testing.....	35
3.8. Density Testing	36
4. RESULTS AND DISCUSSION.....	38
4.1. Density Testing Results.....	38
4.2. Flexural Testing Results.....	40
4.3. Impact Testing Results	42
4.4. Tensile Testing Results	46
4.4.1. <i>Comparison of experimental results to theoretical results</i>	48
4.5. Vibration Testing Results.....	52
4.6. Industrial Application.....	54
5. CONCLUSIONS AND FUTURE WORK.....	62

REFERENCES 65

LIST OF TABLES

<u>Table</u>		<u>Page</u>
1.	Processed Panels Ply Stacking.....	30
2.	Calculated Composite Densities and Corresponding Fiber Volume Fractions	38
3.	Flexural Sample Thickness and Maximum Applied Loads	42
4.	Material Properties Used in Preliminary Study	57

LIST OF FIGURES

<u>Figure</u>	<u>Page</u>
1. Flax, hemp, sisal, wood, and other natural fibers used to make various composites in the Mercedes-Benz E-Class [10].	5
2. Bast fiber structure [17].	6
3. The architecture of an elementary fiber [16].	7
4. Natural fiber's nonlinear elastic tensile behavior with linear fitted trend line.	8
5. Arrangement of carbon atoms in a graphite crystal [22].	10
6. A 3D representative model of the internal structure of a carbon fiber [23].	11
7. Synthetic fiber's linear elastic tensile behavior with linear fitted trend line.	12
8. Basic VARTM schematic.	13
9. The different composite scales [26].	14
10. Comparison between the experimental and ROHM tensile modulus of hybridized composites [6].	24
11. Experimental modulus compared against RoHM and Halpin-Tsai [7].	25
12. Stress distribution schematic for flexure loading.	31
13. Typical VARTM process with caul plate (left) and without caul plate (right).	32
14. Reihle impact test machine (left) and an impact specimen placed in the holder prior to impact (right).	34
15. Vibration analysis set-up.	35

16.	Change in composite density based on fiber volume fractions.....	39
17.	Fiber volume projection chart based on pre-processing fiber weight ratios.	39
18.	Tangent modulus with respect to flax fiber volume fraction.....	40
19.	Ultimate flexural stress versus flax fiber volume fraction test results.....	41
20.	Impact energy versus flax fiber loading results from Charpy impact testing.	43
21.	A plain flax fiber composite’s side profile after an impact event (scale is in centimeters).....	43
22.	A Plain carbon fiber composite’s side profile after an impact event (scale is in centimeters).....	44
23.	The debonding of the flax fiber ply from the carbon fiber ply (Vertical view (left) and horizontal view (right)) (scale is in centimeters).	45
24.	A low flax fiber volume fraction hybrid composite’s side profile after an impact event (scale is in centimeters).	46
25.	Chord modulus of elasticity versus flax fiber loading results.....	47
26.	Tensile stress distribution in hybrid flax carbon composites.....	47
27.	Ultimate stress versus flax fiber volume content test results.....	48
28.	A comparison of the chord modulus of elasticity values obtained experimentally and theoretically.....	49
29.	Coefficient of variance in different theoretical models versus flax fiber volume.....	50
30.	Linear and nonlinear elastic tensile behavior of composites determined through coefficient of determination values.	51

31.	Damping ratios obtained from the single cantilever beam vibration test.	52
32.	Damping ratios of different materials.	53
33.	Raw data from a single cantilever test of plain carbon and plain flax composites.....	54
34.	Agricultural sprayer boom.	55
35.	AGCO hybridized sprayer boom concept design.	56
36.	Preliminary study performed to determine fiber volume fractions necessary for obtaining a greater tensile stiffness than 6061 aluminum.	58
37.	Preliminary study performed to determine fiber volume fractions necessary for obtaining a lower density than 6061 aluminum.	58
38.	Processing T-shaped cross-members using VARTM.	59
39.	Fiber stacking sequence for T-shaped composite cross-members (left) and the finished product (right).	60
40.	Finished AGCO prototype for the adhesively bonded unit cell. Unit cells using aluminum (left) and hybridized carbon and hemp (right) T-braces.....	61

1. INTRODUCTION

1.1. Overview of Hybridized Composites

Composite materials are continually becoming a more attractive choice of material in various industrial applications as a result of their high strength-to-weight and high stiffness-to-weight ratios. Some of the major industries that are driving the transition from traditional materials to composite materials are the aerospace and automotive industries; however there has lately been an increasing use of composite materials in sporting goods as well as in civil infrastructure. These industries' products can exhibit large gains in performance as a result of the weight reduction commonly found from implementing composite materials.

While composite materials offer significant gains in performance as a result of their unique ability to be tailored towards a specific application, they can also offer a means of incorporating biobased materials into a product. This is through the use of natural fibers as reinforcing agents in composites. Due to an increasing demand for biosustainability and a reduction of our current carbon footprint, there has been an increase in the research and development of renewable materials [1].

Natural fibers, when compared to their synthetic or mineral-based counterparts, generally have lower mechanical properties. These low mechanical properties are a major inhibitor when trying to developing high performance products. One method for increasing their level of mechanical performance is to hybridize natural fibers with synthetic fibers or mineral based fibers. The benefit of using hybrid composites is that the advantages of one type of fiber can

overcome the disadvantages of the other type of fiber. As a result, a balance in cost, performance, and sustainability could be achieved through proper composite material design.

When discussing hybrid composites, the hybrid effect is often mentioned. The hybrid effect is used to describe the changes in properties of a composite containing two or more types of fibers, which can either be a positive or negative deviation of a certain mechanical property [1]. The hybrid effect is an important design consideration when determining the desired characteristics of the final composite product.

Natural fibers are most commonly hybridized with glass fibers. Several researchers have found improved mechanical properties from hybridizing natural fibers with glass fibers. The mechanical gains often found from hybridizing fibers ranges from tensile [2, 3, 4], flexural [2, 4, 5], impact [2, 3], as well as others.

The research of H.P.S. Abdul Khalil and associates explored the effect of combining glass fibers with oil palm fibers in a polyester resin. Through their research they were able to observe a positive hybrid effect on mechanical properties. Tensile modulus with an incorporation of 30-70% weight fractions saw steady gains from 3.4 to 4.9 GPa. With small gains of glass fiber (30% weight fractions) there were gains of 150% in flexural modulus, 100% in impact strength, and 100% decrease in water absorption [2].

The work of S. Mishra and associates examined the level of mechanical performance that could be achieved with the incorporation of glass fibers in a biofiber reinforced polyester composite. The biofibers used were pineapple leaf fibers (PALF) and sisal fibers. Through their work, they were able to show a positive hybrid effect with the improved tensile, flexural, and impact properties of both the PALF and sisal fiber reinforced polyester composites with the

incorporation of glass fibers [3]. The gains they found from the incorporation of small amounts of glass fiber with PALF were: 66% improved tensile strength (8.6% glass fiber weight), 34% improved impact strength (8.6% glass fiber weight), and 35.3% flexural strength (4.3% glass fiber weight) [3]. With the inclusion of small amounts of glass fiber with sisal fibers were a 34% increase in impact strength (8.5% glass fiber weight) and a 25% flexural strength improvement (2.8% glass fiber weight) [3]. There was also a decrease of 7% water absorption for hybridized composites when compared to unhybridized composites [3].

While hybridizing is commonly referred to as the combining of natural fibers with glass fibers, hybridizing can also be performed by combining different synthetic fibers together or by combining different natural fibers together. Several researchers have looked into the combining of different types of natural fibers to form hybridized natural fiber composites [6, 7]. Both studies found a positive hybrid effect in mechanical properties by the addition of a stronger or longer fiber to the composite, such as gains in tensile modulus such as a 48% improvement with a 50 wt% inclusion of sisal fibers to banana fibers [6] also a 10% improvement with a 20% inclusion of kenaf fibers to wood flour [7].

While there are many different possible fiber combinations, for high stiffness applications the combination of flax and carbon fibers was explored in this study. The hybridization of flax and carbon fiber offers a good potential for developing high stiffness composites for various structural applications while simultaneously incorporating bio based materials into a product.

1.2. Natural Fibers

Based on an increased awareness that the world's petroleum supply will eventually be depleted, engineers are now beginning to turn towards natural fibers as a means of reducing our

dependency on petroleum based products [8]. A result of this increased awareness, many different natural fiber types are being explored and evaluated. Natural fibers provide many benefits such as specific properties which are comparable to glass fibers but can be produced at 20-40% of the production energy required for synthetic fibers [1, 9]. Natural fibers are broken down into six different groups. The natural fiber groups are as follows: bast fibers (jute, flax, hemp), leaf fibers (sisal and pineapple), seed fibers (coir and cotton), core fibers (kenaf, help, and jute), grass and reed fibers (wheat, corn, and rice), and all other remaining types (wood and roots) [8].

Natural fibers possess many different advantages when compared to synthetic or mineral-based fibers such as good specific strength, good specific modulus, low densities, lower cost, and are bio-based. These benefits are most greatly noticed when the applications are in areas where weight is a concern, where natural fibers have approximately a 40% lower fiber density than glass fibers [10]. Two industries where weight savings are found to result in increased performance characteristics are the automotive industry and the sporting goods industry. An example of natural fibers being used in composite materials is the Mercedes E-Class which can be seen below in Figure 1. The Mercedes E-Class utilizes a wide variety of natural fibers including flax, hemp, sisal, and other natural fibers in the production of over 50 composite components [10].

Natural fibers offer many advantages as well as several drawbacks which must be considered when incorporating them into composites. Several drawbacks to using natural fibers are their high moisture absorption, inferior fire resistance, and low mechanical properties [1]. Natural fibers are also susceptible to high mechanical property variation as a result of varied growing climates, harvesting conditions, and other properties [1]. Natural fibers also exhibit poor

adhesion to various matrices; however this can be improved by incorporating different fiber treatments prior to matrix infusion [11].



Figure 1. Flax, hemp, sisal, wood, and other natural fibers used to make various composites in the Mercedes-Benz E-Class [10].

One issue that often arises when dealing with natural fibers as a reinforcing agent in composites is their inherent mechanical variability [1]. There are several factors which can lead to mechanical variability, these are: crop variety, seed density, soil quality, fertilization, field location, fiber location on the plant, climate, weather conditions, harvest timing, fiber handling and extraction methods, and drying processes [12, 13]. In addition to the previously mentioned items, variation in the cross-sectional area along the length of the fiber also leads to mechanical variation [14, 15].

In order to understand some of the reasons associated with mechanical variability in natural fibers, it is important to understand the architecture of the fiber. The flax fiber starts with a stem, which is comprised of bast fiber bundles. These bundles contain groups of elementary fibers which in themselves contain microfibrils. So when working with bast fiber, the term

“fiber” is actually used to describe a bundle of elementary fibers which consist of several single fiber divisions [16]. The breakdown of a bast fiber can be seen in Figure 2. When discussing elementary fibers, a good way to view them is as a hollow composite [16]. Cellulose fibrils act as the reinforcements, while the hemicelluloses, lignin, pectin, and other amorphous components make up the matrix which holds the cellulose fibrils together [16]. The amounts of these chemical constituents vary by species, strain, and other aspects of a particular plant’s genetics, which leads to varied performance and structure development in different plant fibers [16].

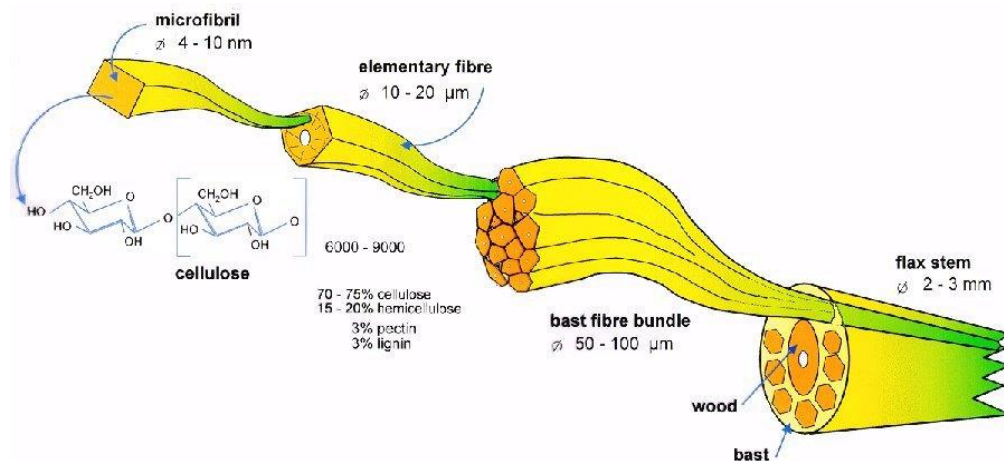


Figure 2. Bast fiber structure [17].

In a single fiber (elementary fiber), there are several different layers that make up the fiber’s structure which are the primary wall, secondary wall (S1, S2, and S3), and the center lumen from outside to inside [18]. Continuing with the concept of a fiber being thought of as a composite, the different layers can be considered different plies within the composite. The architecture of a single fiber can be seen below in Figure 3. The primary wall is the first layer deposited, which contains hemicelluloses and cellulose fibers during the cell growth encircling the secondary walls [19]. The secondary cell wall consists mainly of helically wound cellulose

microfibrils. These microfibrils are made up of 30-100 cellulose molecules [16]. These microfibrils have a diameter of about 10-30 nm [16]. The cellulose microfibrils are responsible for providing the mechanical strength of the fiber [16]. The secondary wall's S2 layer is the thickest layer and contributes approximately 70% of the entire fiber's Young's modulus [20].

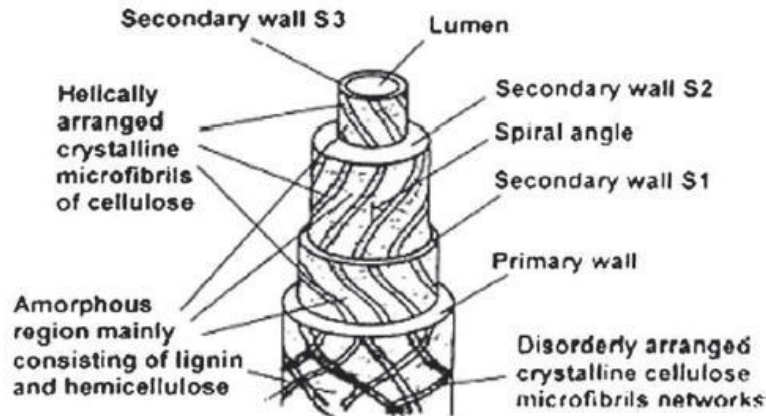


Figure 3. The architecture of an elementary fiber [16].

The microfibrillar angle between the fiber's axis and the microfibril depends on the species of fiber. The microfibrillar angle along with the S2 layer are largely responsible for the mechanical properties of the fiber, where a small angle generally results in higher fiber strength and modulus [8, 15]. The outermost layer consists of pectin and lignin which compile and bind the fiber bundles together yield the final plant structure. The pectin and lignin in these layers reduce the mechanical properties of the fiber in addition influencing the interfacial properties between the fibers and matrix used in the processing of a composite [16].

When using natural fibers it is important to understand that unlike synthetic or mineral based fibers, natural fiber exhibit nonlinear elastic tensile behavior. Figure 4 shows the nonlinear elastic behavior of a flax fiber and epoxy composite during a tensile test. The nonlinear elastic

behavior is the result of the natural fiber's structure. The multiple layers (primary and secondary walls) that make up the natural fiber's structure cause the viscoelastic behavior.

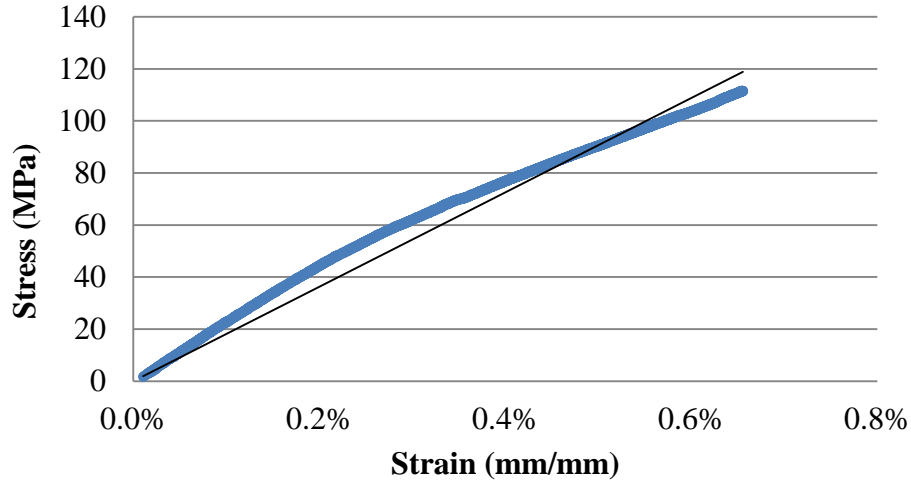


Figure 4. Natural fiber's nonlinear elastic tensile behavior with linear fitted trend line.

The natural fiber under review, flax (*linum usitatissimum*), resides in the bast fiber group [8]. Flax fibers are widely used in biocomposites as a result of their high stiffness, tensile strength, and low density. Flax fibers are grown in temperate regions such as: Netherlands, France, Spain, Russia, Belgium, China, India, Argentina, Canada, and the United States [16]. Flax is also the oldest textile known and is an important standard for the modern textile industry [16]. The plant can grow between 80 and 150 cm in roughly 80 to 110 days, where after which approximately 75% of the plant's height can be used to produce fiber [12]. Currently about 830,000 tons of flax are produced every year [18].

1.3. Carbon Fibers

Carbon fibers are a predominant high-strength, high-modulus reinforcement used in the fabrication of high-performance polymer-matrix composites. While carbon fibers offer high

mechanical properties, their high prices have primarily limited them to aerospace applications where weight savings is considered more critical than costs, however other weight savings industries have also used them in applications where consumers are willing to spend the extra money for weight savings. It was not until the 1990's when the use of carbon fibers had seen a significant increase as a result of a significant price reduction and increase in availability [21]. The price reduction along with the increase in availability resulted in the expanded usage of carbon fiber from predominantly aerospace applications to sporting goods, automotive, civil infrastructure, as well as many other applications.

Carbon fibers are a commercially available fiber with a variety of tensile modulus values which range from 207-1035 GPa [22]. As a general rule, the lower modulus fibers possess lower densities, lower cost, higher tensile and compressive strengths, and higher strain-to-failure than their higher modulus counterparts [22]. Some of the advantages that carbon fibers have over other fibers are: very high tensile strength-to-weight ratios, very high tensile modulus-to-weight ratios, low coefficient of thermal expansion, high thermal conductivity, and high fatigue strength [22]. While some of the disadvantages to carbon fibers are: low strain-to-failure, low impact resistance, high electrical conductivity, and high costs [22].

Carbon fibers are manufactured by treating organic fibers (precursors) with heat and tension, which leads to a highly ordered carbon structure [23]. The most commonly used precursors are rayon-based fibers, polyacrylonitrile (PAN), and pitch [23]. There are advantages and disadvantages for using a specific precursor. PAN-based carbon fibers are lower in cost and have good mechanical properties [21]. They are the dominant class of carbon fiber for structural applications which are widely used in military aircraft, missiles, and spacecraft structures [21]. Pitch-based carbon fibers generally have higher stiffness and thermal conductivities, these

properties make them useful in satellite structures and thermal-management applications [21]. Rayon-based carbon fibers have low thermal conductivity which makes them useful for insulating and ablative applications such as rocket nozzles, missile reentry vehicles nosecones, and heat shields [21].

The strength of carbon fiber comes from its structure which can be seen below in Figure 5. Carbon fibers are formed from planes of carbon atoms connected through strong covalent bonds [22]. These carbon fiber planes are then stacked together and connected through van der Waals bonds, which are much weaker than covalent bonds [22]. As a result of these weaker van der Waals bonds, carbon fibers are very anisotropic mechanical and physical properties.

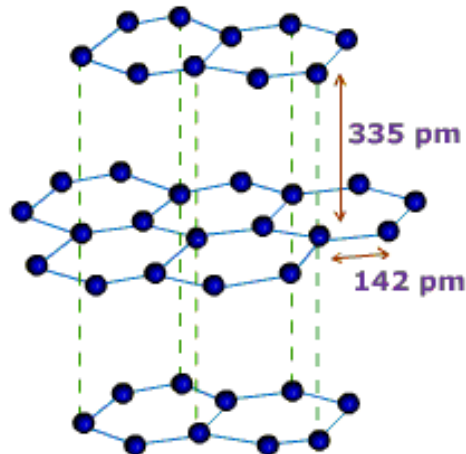


Figure 5. Arrangement of carbon atoms in a graphite crystal [22].

The mechanical properties of a carbon fiber are dependent on the overall structure of the carbon fiber. A carbon fiber can be broken down into two primary sections, the core and the peripheral zone. The peripheral zone is comprised of highly organized stacked graphitic planes. The core of the carbon fiber is made up of basal layers in the longitudinal direction which are twisted and bent. The crystallographic basal planes parallel to the fiber axis can achieve a higher

degree of orientation through a fiber drawing process [22]. Once an increased orientation is obtained an increase in longitudinal strength and modulus will result [22]. The structure of a carbon fiber can be viewed in Figure 6.

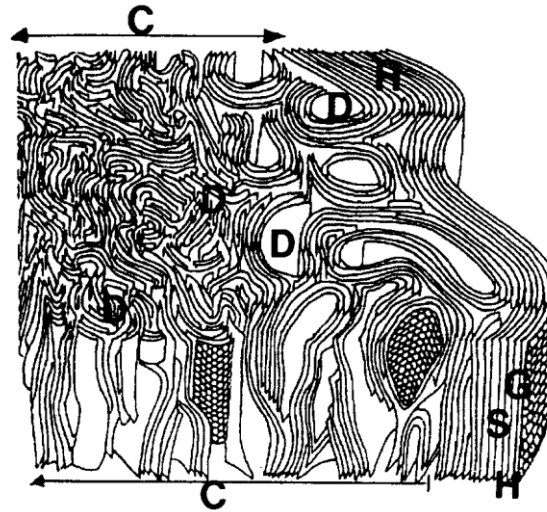


Figure 6. A 3D representative model of the internal structure of a carbon fiber [23].

Synthetic fibers have a linear elastic tensile behavior. Figure 7 shows a carbon fiber and epoxy resin composite during a tensile test. It can be observed that strong linear elastic tensile behavior is obtained when synthetic fibers are used; this is the result of carbon fiber's structure where tensile testing in the fiber direction applies the load to the covalent bonds of the carbon fiber.

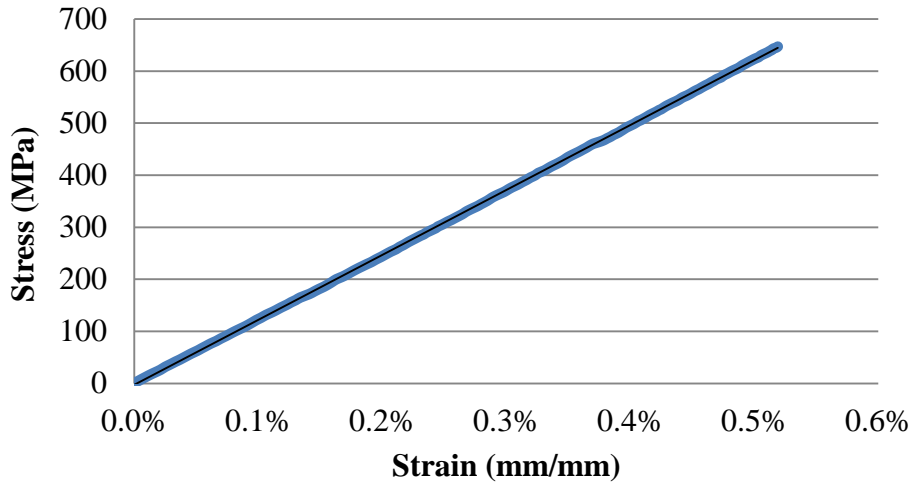


Figure 7. Synthetic fiber's linear elastic tensile behavior with linear fitted trend line.

1.4. Vacuum Assisted Resin Transfer Molding

Vacuum assisted resin transfer molding (VARTM) is a low-cost method for manufacturing large complex composite parts for civil and defense applications [24]. VARTM has many advantages over other manufacturing methods such as resin transfer molding (RTM) such as lower tool cost by eliminating the costs associated with matched-metal tooling, reduced volatile emission, as well as lower injection pressures [25].

The VARTM process is usually conducted in three steps: lay-up of fiber preform, impregnation of the preform with resin, and curing of the impregnated perform. The process uses one solid tooling surface, while the other surface is a formable vacuum bagging film. The resin infusion process is driven by a vacuum pump connected to an outlet port which creates negative pressure gradient to cause resin, entering through the inlet ports, to flow across the preform. For parts that have low permeability a distribution media is often used to help achieve full wet-out of the composite. The time for infusion is a function of resin viscosity, the preform permeability,

and the applied pressure gradient [25]. A schematic for a basic VARTM set-up can be viewed below in Figure 8.

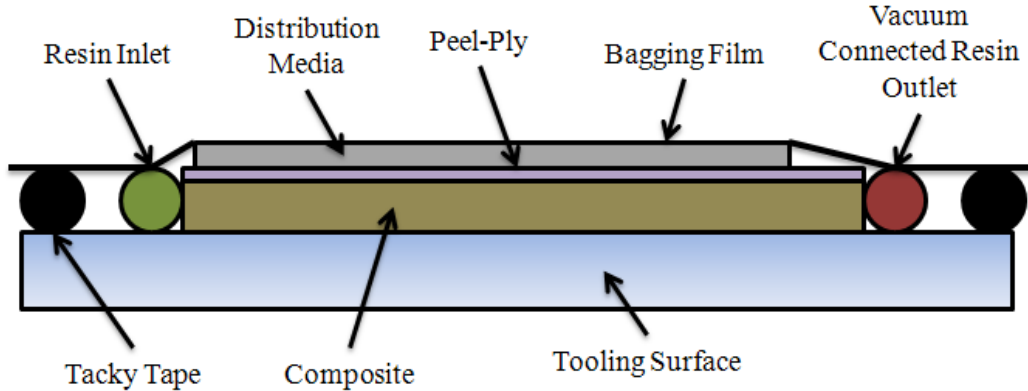


Figure 8. Basic VARTM schematic.

1.5. Modeling Theory

As composite materials are gaining popularity in industry, it is important that engineers have the necessary tools to properly predict the mechanical characteristics of their designed products. Several models have been developed in order to provide mechanical property prediction based on the various composite configurations. While none of these models provide a perfect prediction, many have been proven to show good agreement when compared with experimental results.

There are several different types of reinforcement that can be used to strengthen a material. The two primary types are particulate and fiber reinforcements. Composite materials that are reinforced by fiber are widely used in engineering structures and components. Composite materials can be viewed on many different scales, such as those displayed in Figure 9. The scope of this research however, deals primarily with the microscopic scale. It is at the microscopic

level that several different approach methods for predicting the elastic properties of composites materials can be used. The prediction methods that will be examined are the mechanics of materials and semi-empirical approaches which deal with continuous unidirectional fibers.

The mechanics of materials approach is based on simplifying assumptions of either uniform strain or uniform stress in the constituents [26]. This method is also commonly referred to as the rule of mixtures. This method has been found to adequately predict the longitudinal properties such as Young's modulus (E_1) as well as the major Poisson's ratio (ν_{12}) [27]. The benefit of this method compared with semi-empirical method is that the composite properties are not sensitive to the fiber shape or the distribution of fibers. However, one of the drawbacks to this method is that it underestimates the transverse and shear properties such as the transverse modulus (E_2) and shear modulus (G_{12}) [26].

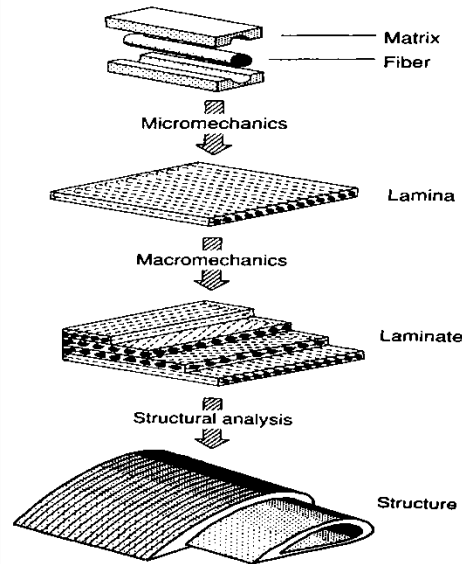


Figure 9. The different composite scales [26].

Semi-empirical relationships, also known as the Halpin-Tsai relationships, have a consistent form for all properties and represent an attempt at carefully interpolating between the

series and parallel models used in mechanics of materials approach which will be discussed later on. This is expressed in terms of a parameter ζ , which is a measure of the reinforcing efficiency (or load transfer), which can be determined through experimental means [26].

In composite materials, the amount of fiber as well as the fiber's mechanical properties is what primarily dictates the properties of the composite. As a result, the longitudinal properties associated with loading in the fiber direction are heavily dominated by the fiber properties which are generally stiffer, stronger, and have lower ultimate strains. If loading occurs in the transverse direction (perpendicular to the fiber direction), the matrix properties are the dominating factor in the overall composite properties. Transverse loading often results in lower stiffness, but improved ductility.

1.5.1. Rule of mixtures model

1.5.1.1. Derivation

A unidirectional composite can be modeled by assuming fibers to be: uniform in properties and diameter, continuous, and parallel throughout the composite [22]. The assumption that perfect bonding exists between the fibers and matrix is also made which implies that there is no slippage occurring at the interface as well as the strains experienced by the fiber, matrix and composite are equal, such that:

$$\varepsilon_c = \varepsilon_f = \varepsilon_m \quad (1)$$

Where the subscripts c, f, and m represent the composite, fiber, and matrix respectively.

The load carried by the composite is shared by the loads carried by the fiber and the matrix such that

$$P_c = P_f + P_m \quad (2)$$

Modifying Equation 2 to represent the corresponding stresses in each constituent based on their respected cross-sectional areas

$$P_c = \sigma_c A_c = \sigma_f A_f + \sigma_m A_m \quad (3)$$

and solving for the stress in the composite

$$\sigma_c = \sigma_f \left(\frac{A_f}{A_c} \right) + \sigma_m \left(\frac{A_m}{A_c} \right) \quad (4)$$

Because the fibers are continuous and parallel throughout, the volume fractions are equal to the area fraction such that

$$V_f = \frac{A_f}{A_c} \quad V_m = \frac{A_m}{A_c} \quad (5)$$

Plugging Equation 5 into Equation 4 results in

$$\sigma_c = \sigma_f V_f + \sigma_m V_m \quad (6)$$

Differentiating Equation 6 with respect to strain, which as previously discussed is that same for the composite, fiber, and matrix, results in

$$\frac{d\sigma_c}{d\varepsilon} = \frac{d\sigma_f}{d\varepsilon} V_f + \frac{d\sigma_m}{d\varepsilon} V_m \quad (7)$$

Where the derivative of stress with respect to strain represents the slope of the corresponding stress strain curve, which if linear, is equal to the elastic modulus. Thus

$$E_c = E_f V_f + E_m V_m \quad (8)$$

Equation 8 can be generalized into the following equations

$$\sigma_c = \sum_{i=1}^n \sigma_i V_i \quad (9)$$

$$E_c = \sum_{i=1}^n E_i V_i \quad (10)$$

Which indicate that the contributions of the fibers and the matrix to the average composite properties are proportional to their respective volume fractions. The derived relationships in Equations 9 and 10 are called the rule of mixtures.

As previously stated, when the loading of the composite is in the direction of the fibers such as is in tension, the rule of mixture's model predictions are in good agreement with those obtained experimentally. However, when a compressive load is applied the experimental values deviate from the predicted values [21]. This is a result of the fibers behaving similarly to columns on an elastic foundation, which results in the compressive response of the composite being dependent on the matrix compressive properties [21].

1.5.1.2. Factors effecting actual composite properties

As previously discussed, several assumptions were made during the derivation of the rule of mixtures. These assumptions however can play a large role in the actual composite strength and stiffness. The factors which can influence the composite properties are: fiber misalignment, discontinuous fibers, interfacial bonding, and residual stresses.

1.5.1.3. Fiber misalignment

Orientation of fibers with respect to the direction of the loading axes is an important parameter and has a direct effect on the load transfer between the fibers and the matrix. Maximum fiber loading is only achieved when the fibers are parallel to the loading axis, so misalignment of fibers can result in an overall decrease in the load bearing capacity of the

composite. When looking at bast fiber, the variation of the fibril angle in the secondary wall can also be considered fiber misalignment within the sub-composite. This variation in the fibril angle can also be a source of error when using the rule of mixtures.

1.5.1.4. Discontinuous fibers

Discontinuous fibers cause stress concentrations at the end of the fiber [28]. This is particularly important in composite failure when the matrix is brittle. The reason for this is even at small composite loadings, the fiber ends will become separated from the matrix which results in the formation of microcracks in the matrix. The same effect occurs in continuous fibers when a fiber breaks. Once microcracks have formed there are several things that can happen. The first scenario that can occur is that the crack can propagate along the length of the fiber which will render the fiber ineffective and the composite will act as a bundle of fibers, where the matrix is no longer aiding in strengthening the composite [28]. The alternate scenario that can occur is that the crack will propagate normal to the fiber direction. Once this occurs, the crack will run into other fibers which will create another stress concentration that will eventually result in composite failure [28]. When dealing with bast fibers, discontinuous fibers can be a problem. During processing and separation, many elementary fibers are still intact with their bundles and therefore appear longer while others are separated into elementary fibers which are quite short compared to when they are still in bundles.

1.5.1.5. Interfacial bonding

The interface between fibers and matrix is important because of its role in transferring stress from one constituent to the other. The interfacial bonding between the matrix and the fibers can be broken down into two different levels of interaction, the molecular level and the

micro level. The molecular level is considered the most basic level, where at this level the interactions between the matrix and fiber are determined by the chemical structures of both phases and is due to van der Waals forces, acid-base interactions and chemical bonds [29]. From a chemical stand point, the strength of interfacial interactions depends on the surface concentration of interfacial bonds and the bond energies [29]. At the micro-level, where the interfacial interactions are usually described by the various parameters which characterize the load transfer through the interface which include: interfacial shear stress, bond strength, and critical energy release rate [29].

The bonding between the matrix and fibers becomes increasingly important when an individual fiber fractures prior to the ultimate failure of the composite [21]. The reason for this is because the strength of the bond determines the mode of propagation of microcracks at the fiber ends. When a strong bond is present between the fibers and the matrix, the cracks do not propagate along the length of the fibers. This means that the load transfer from the matrix and the fiber is still present and the fiber is still a viable reinforcement. A strong bond also results in higher transverse strengths and for improved environmental performance such as water resistance [30].

Poor interfacial bonding between matrix and fiber is a common problem when dealing with natural fibers. Natural fibers are hydrophilic and often suffer from high moisture absorption while many polymers are hydrophobic which creates a high degree of incompatibility between fiber and resin [8, 11]. In addition to dissimilarities in polarity between matrix and fiber, the surface quality of natural fibers also presents adhesion issues. Natural fiber surfaces are often covered in lignin, wax, and oils which cause poor bonding sites for polymer matrices [8]. There are however different techniques being explored in order to resolve these problems. Many of

these techniques involve the altering of the fiber's surface to provide more bonding sites for the polymer through chemical methods [8, 11].

1.5.1.6. Residual stresses

The manufacturing process of fiber reinforced composites often results in the creation of residual stresses within the composite. These residual stresses are the result of the different thermal expansion coefficients of the composite constituents [31]. These stresses are especially apparent in laminates with different angled plies. High residual stresses can also occur in composites with different reinforcing fiber types with a mismatch in coefficients of thermal expansion.

1.5.2. Halpin-Tsai model

The Halpin-Tsai equations are based on the self-consistent micromechanics method which was developed by Hill [32]. The modulus values obtained from the Halpin-Tsai equations agree reasonably well with the experimental values for various reinforcing geometries such as fibers, flakes, and ribbons.

In its general form it can be written as

$$P^* = \frac{P_m(1+\xi\eta V_f)}{1-\eta V_f} \quad (11)$$

Where

$$\eta = \frac{P_f - P_m}{P_f + \xi P_m} \quad (12)$$

and P^* is a composite property ($E_{11}, E_{22}, G_{12}, G_{23}, \nu_{23}$), ξ is the reinforcing efficiency which can be measured experimentally. ξ is effected by reinforcement geometry, packing geometry and loading conditions [32]. P_m and P_f are the matrix property and fiber property respectively.

When determining ξ through experimental means, the following equation is used:

$$\xi = \frac{P_f(P^* - P_m) - V_f P^*(P_f - P_m)}{P_m[(P_f - P^*) - V_m(P_f - P_m)]} \quad (13)$$

where V_f and V_m the fiber volume fraction and matrix volume fraction, respectively.

As ξ approaches infinity, Equation 24 takes the form,

$$\xi = V_f P_f + V_m P_m \quad (14)$$

which is similar to the rule of mixtures equation previously discussed. This model is known as the parallel model or the Voigt model [21]. This model has high fiber dependency when determining composite properties.

As ξ approaches zero, Equation 24 takes the form,

$$\xi = \left(\frac{V_f}{P_f} + \frac{V_m}{P_m} \right)^{-1} \quad (15)$$

This form of the equation is known as the series model or the Reuss model [21]. This model has a high dependency on the matrix properties when determining the composite properties.

The Halpin-Tsai equation can also be used in hybridized fiber scenarios. When hybridized fiber cases are used, the equation to use is,

$$P_{hybrid\ Composite}^* = P_{Fiber\ 1}^* + P_{Fiber\ 2}^* \quad (16)$$

The hybrid composite properties ($P_{hybrid\ Composite}^*$) are determined by performing the Halpin-Tsai equations for a single fiber single matrix equation for each fiber type then summing them together at their respective fiber volumes.

Most micromechanical analyses deal with the simplest type of composite which is one consisting of continuous and parallel fibers in a matrix. The properties of unidirectional lamina are not only dependent on the fiber volume ratio but are also dependent on the packing geometry of the fibers. There are three idealized packing geometries which are: rectangular, square, and hexagonal. The maximum fiber volume ratios for the three fiber packing geometries are determined by the fiber radius and the fiber spacing as follows [26]:

Rectangular packing:

$$V_f = \frac{\pi}{4} \left(\frac{r^2}{R_2 R_3} \right) = 0.785 \quad (17)$$

Square packing:

$$V_f = \frac{\pi}{4} \left(\frac{r}{R} \right)^2 = 0.785 \quad (18)$$

Hexagonal packing:

$$V_f = \frac{\pi}{2\sqrt{3}} \left(\frac{r}{R} \right)^2 = 0.907 \quad (19)$$

1.5.3. Rule of hybrid mixtures

In many applications it is beneficial to produce a composite with the inclusion of several different fibers. This type of composite is known as a hybrid. The term hybridization is commonly referred to the combining of synthetic glass fibers with natural cellulose based fibers

[3]. The hybridizing technique is useful for creating a high strength composite while still achieving low density and high biodegradability. While the hybridizing technique is gaining popularity, it is important to be able to predict its mechanical outcomes. One method for doing such theoretical predictions is to use the rule of hybrid mixtures (RoHM).

The rule of hybrid mixtures is similar to the rule of mixtures; however it is mainly used in randomly oriented short fiber applications. The model is derived by first considering a hybrid composite as a system that consists of two single composite systems. It is assumed that these two single systems have no interaction between each other. This assumption is used to obtain the equation

$$\varepsilon_{hc} = \varepsilon_{f1} = \varepsilon_{f2} . \quad (20)$$

Where the subscripts hc, f1, and f2 represent the hybrid composite, fiber #1, and fiber #2 respectively [6]. From there, the modulus of the hybrid composite can be evaluated from the rule of hybrid mixtures equation by neglecting the interaction between the two systems as follows:

$$E_{hc} = E_{c1}V_{c1} + E_{c2}V_{c2} \quad (21)$$

where E_{hc} , V_{c1} , and V_{c2} are the elastic modulus of the hybrid composite, the relative hybrid volume fraction of the first and second systems respectively [6]. The following relations are valid for the assumed system [7]:

$$V_{c1} + V_{c2} = 1 \quad (22)$$

$$V_{c1} = V_{f1}/V_t \quad (23)$$

$$V_{c2} = V_{f2}/V_t \quad (24)$$

$$V_t = V_{f1} + V_{f2} \quad (25)$$

Using these equations, researchers have determined the mechanical trends of hybrid natural fiber composites by varying the volume fraction ratios of banana fibers to sisal fibers [6]. The results they came up with can be observed in Figure 10.

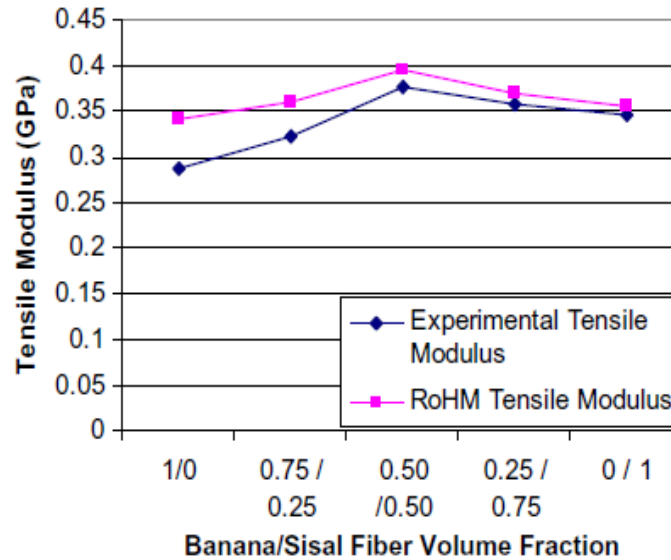


Figure 10. Comparison between the experimental and ROHM tensile modulus of hybridized composites [6].

From their research, they have determined that the rule of hybrid mixtures tends to over predict the tensile modulus. Some of their reasoning for why the rule of hybrid mixtures over predicts the modulus is that microvoids between the fiber and matrix during the processing of the composite have a strong influence [6]. This trend is also supported by researchers who have hybridized wood flour and kenaf fiber in polypropylene, whose modulus comparisons at varying fiber loadings with respect to the rule of hybrid mixtures and Halpin-Tsai model can be seen in Figure 11 [7]. When looking at the Halpin-Tsai model presented in Figure 11, it can be observed that the model under predicts the tensile modulus values at low kenaf fiber loadings (<25 wt%)

but over predicts modulus values at high kenaf loadings (>25 wt%). The authors provide no explanation as to why this trend occurs.

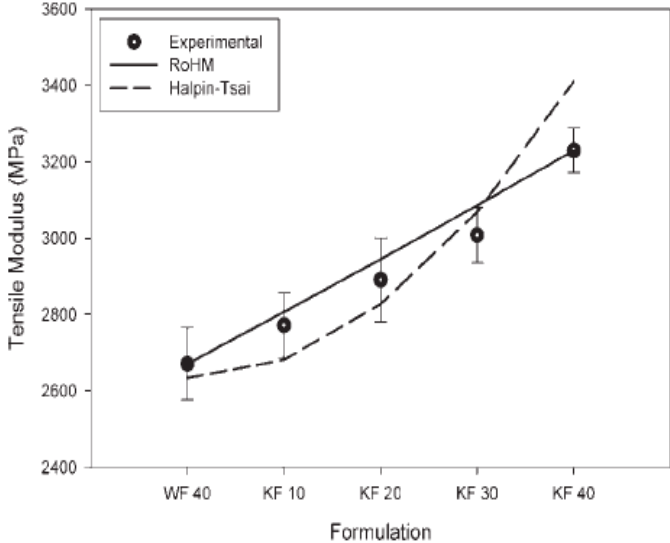


Figure 11. Experimental modulus compared against RoHM and Halpin-Tsai [7].

2. OBJECTIVES OF RESEARCH

Natural fiber composites have been found to exhibit suitable mechanical properties for general applications. However, when high strength applications are required, natural fibers are typically not considered as a practical fiber. Several of the reasons for this are natural fiber exhibit lower mechanical properties than their synthetic counterparts as well as have a high degree of fiber to fiber mechanical variability which lowers their mechanical performance predictability. One potential method for solving natural fiber's shortcomings is to hybridize them with synthetic fibers with the goal of improving composite mechanical properties as well as reducing composite to composite mechanical variability.

While hybridizing natural fibers with synthetic fibers may potentially offer a means of improving composite mechanical properties, it is important to also explore existing modulus prediction models to determine if they are a viable means of property prediction. The most commonly used model for modulus prediction is the rule of mixtures, which has been shown to provide results that are in good agreement to experimental results. While this model is commonly used for a single type of reinforcing fiber, it will be a valuable exploration to establish if it still maintains accurate value prediction for multiple fiber types.

Through hybridizing fibers, the scope of this thesis intends to accomplish the following:

- Combine flax fibers with carbon fibers at varying fiber volume fractions to determine mechanical trends.
- Reduce mechanical property variability inherent in natural fiber composites through hybridization with carbon fiber.

- Compare experimental values to predicted values by using traditional theoretical models such as the rule of mixtures and Halpin-Tsai to determine an accurate method for mechanical performance prediction.
- Increase the renewability content while maintaining significant mechanical properties for load bearing applications.

3. MATERIALS AND METHODS

The materials used in this study for developing hybridized composites were carbon fiber and flax fiber in an epoxy resin matrix. The method used for processing the materials into a composite was vacuum assisted resin transfer molding (VARTM). Once the materials were processed a wide range of mechanical testing was performed in order to determine the mechanical abilities of the hybrid composites. This chapter will discuss: the materials used, the method for processing the materials, and the mechanical testing methods that were performed on the processed composites.

3.1. Carbon Fiber

The carbon fibers used in this study were manufactured by Hexcel Corporation, and can be found under the item name GA130. The carbon fibers come in a unidirectional fabric mat with an areal density of 448 g/m^2 at a fabric thickness of 0.43 mm [33]. When calculating theoretical properties, a published fiber density of 1.80 g/cm^3 was used [21]. The fabric has a tow size is 12k at 14 tows/in with an elastic modulus of 227.5 GPa [33].

3.2. Flax Fiber

The flax fibers used in this study were manufactured from Composites Evolution Ltd. The flax fibers known as Biotex Flax, come in a unidirectional fabric with an areal density of 420 g/m^2 [34]. The flax fibers have a density of 1.5 g/cm^3 and a diameter of $20 \text{ }\mu\text{m}$ [34]. The flax fibers have a tensile modulus of 50 GPa and a tensile strength of 500 MPa [34].

3.3. Epoxy Resin

The epoxy resin system used in this study was manufactured from Huntsman Corporation. The epoxy resin is Araldite LY 8601 which is mixed with Aradur 8602 hardener. The epoxy resin system has a mixing ratio of 4 parts resin to 1 part hardener by weight [35]. It has a 70 minute gel time with a recommended 24 hour demold time [35]. Full cure is obtained after a period of 3 days has been reached [35]. Once fully cured, the epoxy has a density of 1.12 g/cm³ [35]. Some of the mechanical properties are a tensile strength of 54.3 MPa, flexure strength of 75.9 MPa, flexural modulus of 2.22 GPa, and a compressive strength of 106.2 MPa [35].

3.3. Materials Processing

The scope of this project is to determine the effect that increasing the amount of flax fiber has on various mechanical properties of a composite. In order to vary the fiber volume fraction of flax, different carbon and flax fiber weight fractions were used for each panel configuration. This was accomplished by increasing or decreasing the number of flax or carbon fiber plies within a panel, while still maintaining the same fabric layering scheme. The fabric layering sequence was [Carbon/Flax/Carbon/Flax/Carbon]. A plain carbon and plain flax panel were also processed for a baseline comparison of mechanical properties.

As mentioned previously, in order to achieve varied flax fiber volume fractions the weight fractions were varied by controlled by the number of carbon and flax fiber plies used. Table 1 shows the number of carbon and flax fiber plies used for each stacking configuration. It can be observed that when flax fiber plies were added, they were distributed evenly in order to keep the laminate symmetric and balanced. When carbon fiber plies were added, they were

added about the center of the composite. All fibers were aligned in the same direction so that all fibers in the composite were parallel.

Table 1. Processed Panels Ply Stacking

<i>Panel Configuration</i>	<i>Carbon Plies</i>	<i>Flax Plies</i>	<i>Carbon Plies</i>	<i>Flax Plies</i>	<i>Carbon Plies</i>	<i>Carbon:Flax Weight Ratio (Pre-Infusion)</i>
1	1	1	10	1	1	7.41
2	1	1	7	1	1	5.57
3	1	1	4	1	1	3.68
4	1	1	1	1	1	1.79
5	1	2	1	2	1	0.89
6	1	3	1	3	1	0.60
7	1	4	1	4	1	0.46

In order to understand the reasoning behind the layering sequence it is best to look at a flexural loading scenario. In a flexural loading scenario, the stress is not uniformly distributed across the cross-section. Figure 12 shows a basic schematic for a laminate composite under flexural loading. Looking at the figure it can be understood that half the composite is under a compressive stress while the other half is under a tensile stress. However it can also be observed that there is a point in the middle of the composite where there is zero normal stress. The point of zero normal stress is known as the neutral axis, it is at this location that the load switches from tensile to compression or vice-versa. In homogenous materials the stress diagram would have a consistent gradual increase in tension or compression stresses as you move further away from the neutral axis until you reach the maximum stresses at the outer surface. In laminate composites, this is not necessarily the case. Depending on the stacking sequence and materials properties at each ply, the laminate may have jumps in stress distribution such as those observed in Figure 12. Looking specifically at the stacking sequence chosen for this study, by distributing the carbon plies evenly about each carbon layer would create huge gains in flexural modulus as well as

flexural strength as a result of carbon fiber's superior mechanical attributes. By applying the carbon fiber plies centrally (about the neutral axis) this will help dissipate some of gains achieved by obtaining additional carbon fiber plies which will help make the hybridized laminates more comparable throughout the study.

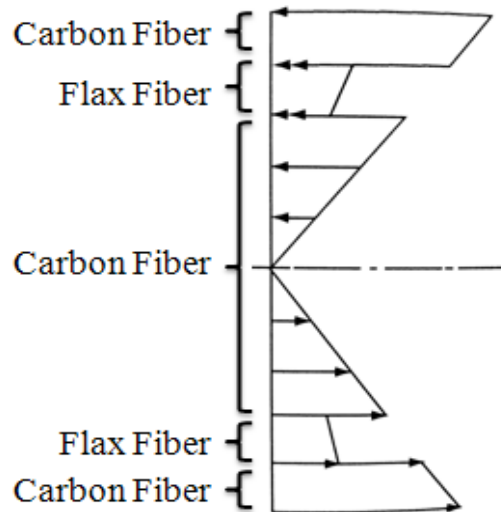


Figure 12. Stress distribution schematic for flexure loading.

Once a stacking sequence was determined, vacuum assisted resin transfer molding (VARTM) was implemented to process all the composites used in the experiments. However, prior to infusion the fabric mats were cut to the proper dimensions and were then placed in an oven at 80°F for a period of 24 hours to dry. While fabric was drying, the VARTM process was set-up. Two different set-ups were used for processing. The first method used a caul plate. The caul plate provided two tooling surfaces as well as a more uniform cross-sectional area across the finished part. The caul plate was used when high amounts of flax fiber were used in the processing such as in parts which had a flax fiber volume of 20% or more. In these scenarios, the flax acted as a distribution media which provided easy resin flow through the composite. The

second set-up was performed without a caul plate as a result of the need for a distribution media. Panels were processed at 304.8 in by 317.5 mm. The two set-ups can be viewed in Figure 13.



Figure 13. Typical VARTM process with caul plate (left) and without caul plate (right).

Once the VARTM process was set-up, the fabric was removed from the oven and flax fiber mats and the carbon fiber mats were each massed separately so the amount of each fiber type going into a panel was known. After the fabric was massed, it was laid into place and the bagging film was secured to the tacky tape. On completion of the bagging process, a vacuum pressure of 165 kPa was drawn from the vacuum pumps. Panels were debulked for 30 min in order to minimize the air trapped within the panels before resin infusion. After the debulking period, the appropriate amount of resin was prepared and infused into the panel. Once the infusion process was complete the inlet port was closed and the panel was allowed to cure for 24 hours.

Once the panel had reached its demolding time, the panel was removed from the table and was then massed. After massing the panel, it was then taken to a wet saw where it was sectioned into the proper dimensions for the various tests that would be performed. In order to maintain consistency in testing results, all mechanical testing was performed from the same

panel. Once the panel had been properly sectioned, the fresh cut test samples were placed into an oven at 80°C for a period of 24 hours to dry and to allow for additional curing.

3.4. Flexure Tests

Flexural testing was performed through a three-point bend testing, as specified in ASTM D790, using an Instron 5567 load frame [39]. The speed of the crosshead was calculated according to the guidelines specified in the standard, which resulted in values that ranged from 4.5 to 11.3 mm/min. 5 specimens were tested for each test sample. The lengths of the specimens were set to accommodate a span-to-depth ratio of 32, which was chosen for all tests as a result of the composite's high-strength reinforcing fibers. The higher span ratio was recommended by the test standard for composites with high-strength reinforcing fibers in order to eliminate shear effects, which can influence modulus measurements.

3.5. Tensile Tests

Tensile testing was performed according to ASTM D3039, using an MTS load frame. 5 specimens were tested for each test sample. The recommended geometry for 0 degree unidirectional composites are 250 mm long by 15 mm wide and thickness is determined by ply stacking lay-up. The use of tabs was also implemented as recommended by the standard for testing highly unidirectional composites to help promote failure within the gage section. Tabs were made from glass fibers and had a geometry of 56 mm long by 15 mm wide and 1.5 mm thick. Samples were tested at a constant cross head displacement of 2 mm/min. Chord modulus calculations were performed between 0.001 and 0.003 mm/mm strain as recommended by the ASTM standard.

3.6. Impact Tests

Impact testing was performed using a Reihle impact test machine. Figure 14 shows the testing apparatus in addition to the specimen holding fixture. The lowest impact weight was used to provide the best resolution which resulted in a maximum potential impact force of 30 ft-lbs. Unnotched specimens were chosen in order to provide more accurate representation of composite behavior under real world impacting scenarios. A minimum of 5 specimen were tested for each sample set, however impact test results had the highest variations so some tests had an increase in sample size to provide a smaller standard deviation. The specimen sizes were selected based on ASTM A370. ASTM A370 was originally written for testing metals and aluminums; however, because there is no standard for Charpy impact tests for composites, the standard was modified to accommodate composite materials. The dimensions called out in the standard were used, which calls for specimens to be 55 mm long by 10 mm wide while the thickness varied based on panel configuration.



Figure 14. Reihle impact test machine (left) and an impact specimen placed in the holder prior to impact (right).

3.7. Vibration Testing

Vibration testing was performed by placing a 25.4 mm wide by 304.8 mm long specimen on top of a cast iron machining block and then placing a block of aluminum on top of the specimen. The specimen was then secured into place by tightening a c-clamp on the outside surfaces of metal pieces. The resulting set-up formed a fixed end cantilevered beam. An Omron Z4M-S40 laser displacement sensor was placed at the tip of the free end and was connected to a data acquisition system. The resulting set-up can be seen in Figure 15. LabView was used to generate voltage versus time plots which were then used to determine vibration characteristics.

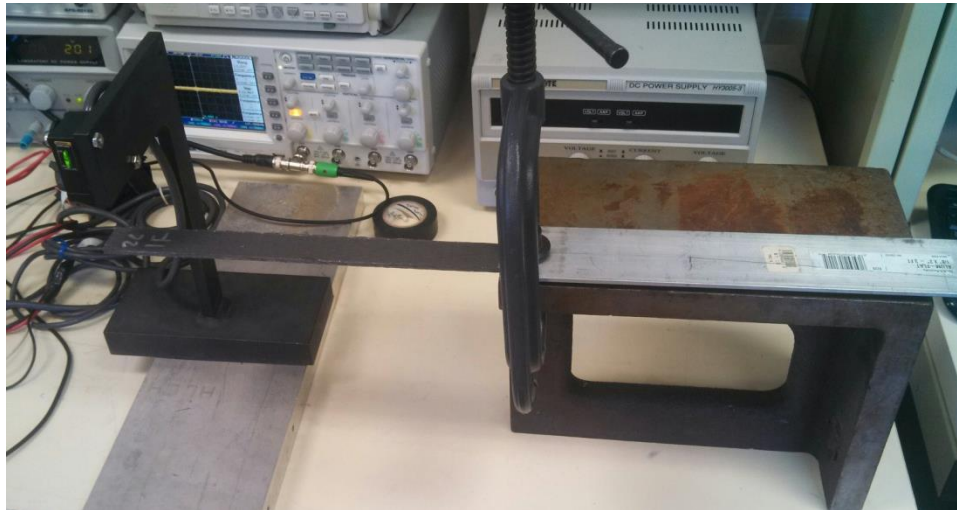


Figure 15. Vibration analysis set-up.

The voltages versus time plots were generated by running LabView, displacing the tip of the sample, and then releasing the sample. The plotted data revealed a sinusoidal wave whose amplitude decreased logarithmically with time. The process was completed three times in order to achieve an accurate sampling set. Two points were selected on the generated plot and then the following equations were used to determine the vibrational damping frequency based on the generated plots.

$$\delta = \frac{1}{2\pi n} \ln \left(\frac{A_1}{A_2} \right) \quad (30)$$

And,

$$\zeta = \frac{1}{\sqrt{1 + \left(\frac{2\pi}{\delta} \right)^2}} \quad (31)$$

Where δ is the log decrement, ζ is the damping ratio, A_1 and A_2 are the amplitudes of the first and last amplitudes measured respectively, and n is the number of cycles in between the measured amplitudes.

3.8. Density Testing

Density testing was performed using a water immersion method. 5 specimens were tested for each test sample. The samples were massed on an Ohaus Adventurer high precision scale. The process consisted of massing the sample dry the massing the sample immersed in water and applying the following equation:

$$\rho_{composite} = \frac{m_{dry}}{(m_{dry} - m_{wet})} \rho_{water} \quad (32)$$

Once the composite density was determined, the fiber volume fractions could then be calculated. Using the fiber masses recorded during pre-processing and the composite mass recorded post processing the mass of the infused resin could be determined. This was accomplished by subtracting the fiber masses from the final composite mass. With all the masses of the constituent materials now known, the weight fractions could then be determined by dividing the mass of the constituent by the mass of the composite. The volume fractions can then be determined by applying the equation below:

$$V_{constituent} = \frac{\rho_{composite}}{\rho_{constituent}} W_{constituent} \quad (33)$$

Through these calculations, a void volume fraction of zero was assumed for all composites.

4. RESULTS AND DISCUSSION

4.1. Density Testing Results

Performing the procedure discussed in the density testing methods section, the fiber volumes and densities for the processed panels were determined. The table below shows the calculated values from the density testing (Table 2).

Table 2. Calculated Composite Densities and Corresponding Fiber Volume Fractions

<i>Panel Configuration</i>		<i>Plain Carbon</i>	<i>1</i>	<i>2</i>	<i>3</i>	<i>4</i>	<i>5</i>	<i>6</i>	<i>7</i>	<i>Plain Flax</i>
<i>Density (comp)</i>	<i>average</i>	1.536	1.448	1.443	1.410	1.310	1.270	1.231	1.230	1.157
	<i>Std. Dev.</i>	0.001	0.009	0.004	0.007	0.009	0.011	0.019	0.010	0.045
<i>Fiber Volume Fractions</i>	<i>Carbon</i>	61%	47%	47%	41%	28%	20%	15%	12%	0%
	<i>Flax</i>	0%	8%	10%	13%	19%	27%	30%	32%	38%
	<i>Total</i>	61%	55%	57%	55%	48%	46%	44%	44%	38%
<i>Weight Fraction</i>	<i>Carbon</i>	71%	59%	58%	53%	39%	28%	22%	18%	0%
	<i>Flax</i>	0%	8%	10%	14%	22%	31%	36%	39%	49%
	<i>Epoxy</i>	29%	34%	31%	33%	39%	41%	42%	43%	51%

The data from the table above was used to generate the figure below (Figure 16). From the figure below, it can be noted that with an increase in flax fiber volume fraction, there is a reduction in composite density which was to be expected as a result of the flax fiber possessing a lower density than carbon fiber. The trend of composite density reduction with an increase in flax fiber loading is strongly linear.

The data obtained from the measurements of weight ratios (pre-processing) and their corresponding fiber volume fractions (calculated post-processing) was used to generate Figure 17. The figure can be used as a guide for targeting specific fiber volume fractions through using weight ratios if additional research is to be carried out after this study is published. The provided

information is only useful when processing hybrid composites using VARTM with a vacuum pressure of 165 kPa. If additional pressure is applied, higher fiber volumes can be obtained; however, this will render the information provided in the figure useless.

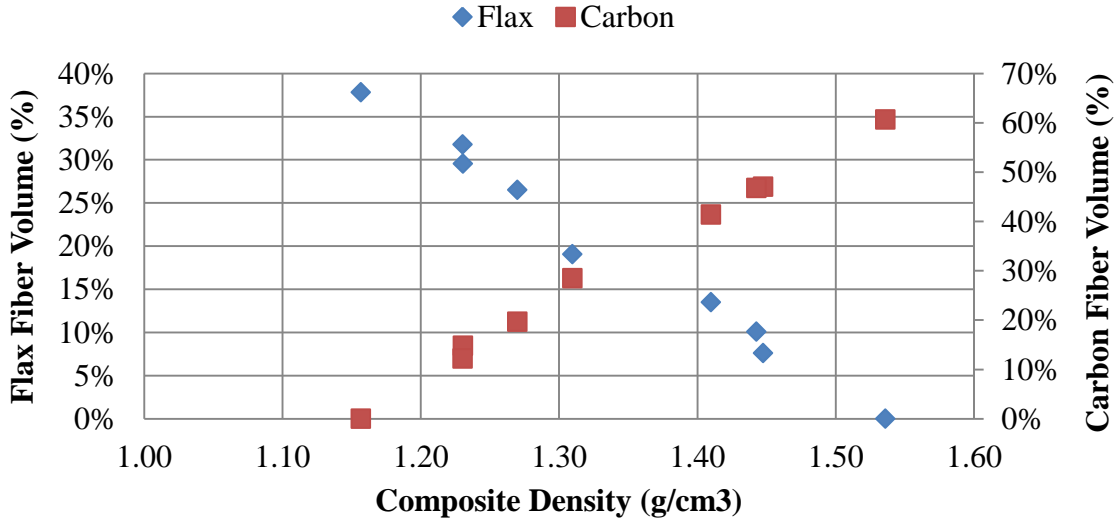


Figure 16. Change in composite density based on fiber volume fractions.

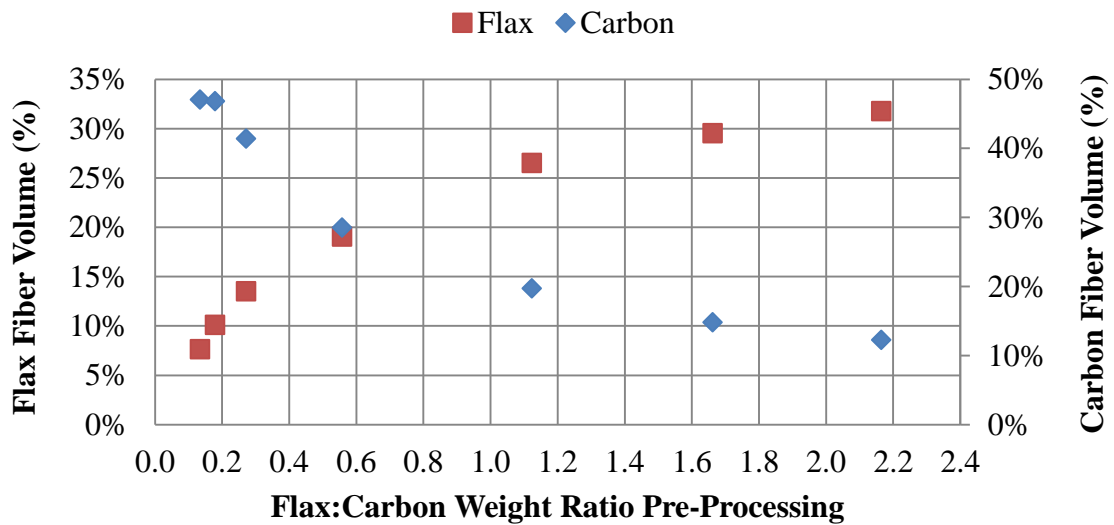


Figure 17. Fiber volume projection chart based on pre-processing fiber weight ratios.

4.2. Flexural Testing Results

Flexural testing was performed on all the processed panels. Figure 18 shows the tangent modulus results from the flexural tests. The samples with the highest tangent modulus were the plain carbon fiber samples, while the lowest tangent modulus samples were found on the other end of the spectrum in the plain flax fiber samples. The second highest tangent modulus is in 20% flax fiber volume samples (configuration 4) which have a stacking sequence of [C/F/C/F/C]. The general trend is that with an increase there is decrease in tangent modulus.

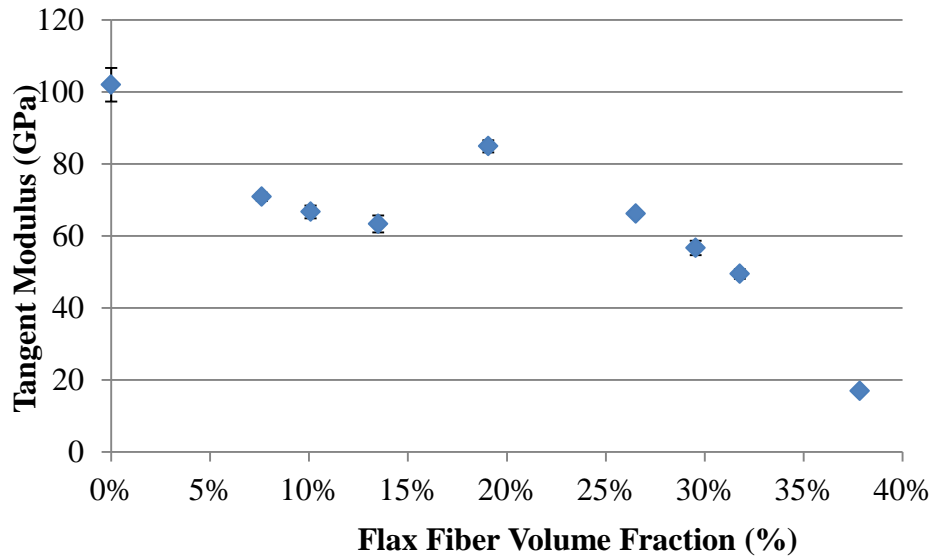


Figure 18. Tangent modulus with respect to flax fiber volume fraction.

The ultimate flexural stress of the tested samples can be seen below in Figure 19. It can be observed that with an increase in flax fiber, there is a decrease in ultimate flexural stress. The primary mode of failure for the hybrid samples was the result of compression failure within the carbon fiber layer. However in the plain flax samples, tensile failure was the dominating failure mode. Similar to the hybrid composites, plain carbon fiber samples were also limited by the compressive strength of the fibers.

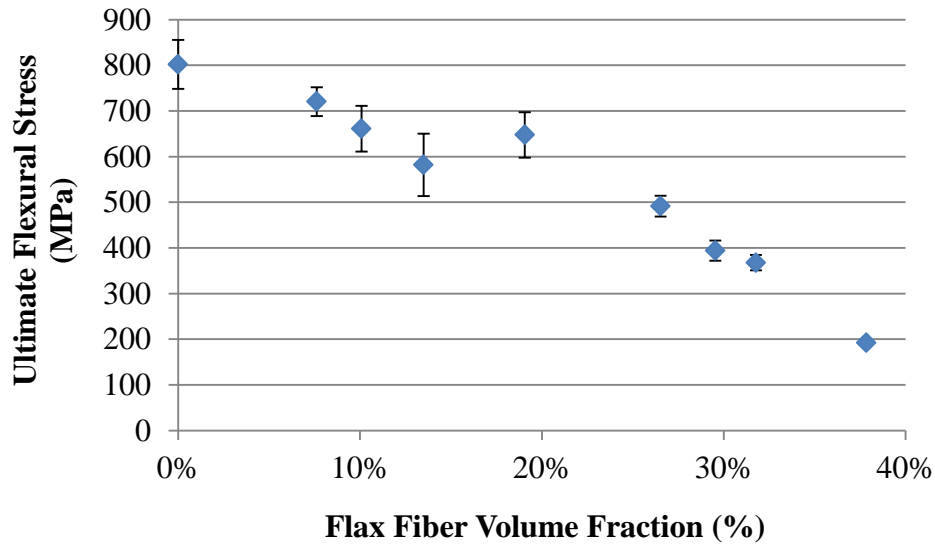


Figure 19. Ultimate flexural stress versus flax fiber volume fraction test results.

In order to understand the modulus trends as well as the flexural strength trends it is important to look at the maximum loads in relation to the sample thicknesses. Table 3 shows the sample thicknesses as well as the maximum loads. Configuration 4 is the simplest lay-up scheme with a stacking sequence of [C/F/C/F/C] which results in the thinnest panel at 2.60 mm. Configurations 3 and 5 double in thickness as a result of the additional plies, however the gain in max load is not doubled. This is because the main source of stiffness and strength are the outside carbon layers which are only 1 ply thick for each panel configuration. The basics of stress distribution under flexural loading in laminate composites was discussed previously in the section 7.3 Materials Processing, which will help shed light on this issue. Configurations 1-3 have increasing carbon fiber plies at the center of the composite, which began to show failure patterns similar to plain carbon. However, the flax fiber layer between the central and outer carbon fiber plies limits the flexural modulus and strength as a result of the low flax fiber flexural properties. From the results, it can be seen that flax fiber provides little in the way of

flexural reinforcement and that fiber stacking sequences play a large role in flexural property performance.

Table 3. Flexural Sample Thickness and Maximum Applied Loads

<i>Panel Configuration</i>	<i>Plain Carbon</i>	<i>1</i>	<i>2</i>	<i>3</i>	<i>4</i>	<i>5</i>	<i>6</i>	<i>7</i>	<i>Plain Flax</i>
<i>Thickness (mm)</i>	3.50	6.80	5.30	4.10	2.60	4.00	5.20	6.50	3.40
<i>Max Load (N)</i>	775.2	1245.2	911.2	623.1	501.4	520.0	533.0	693.3	171.5

4.3. Impact Testing Results

Impact testing was performed on all the processed panels, and the testing results can be seen below in Figure 20. It can be observed that flax by itself has very low impact strength (38.4 kJ/m²). The impact strength of carbon on the other hand, is nearly 820% larger. As previously discussed, through hybridization the low impact strength of plain flax fiber can be greatly improved with the incorporation of carbon fiber. An improvement of over 408% was observed with only the incorporation of a 12% carbon fiber volume fraction.

It can be observed that flax fibers by themselves have relatively low impact strength. One method for explaining the poor impact performance of flax fibers is to look at their failure modes after an impact event has occurred. Figure 21 shows the typical failure mode of flax fiber composite failure. Several failure modes can be observed. The first failure mode is fiber breaking and consequently pullout from the matrix. The second mode is local fiber debonding from the matrix. While these methods all help to dissipate energy during an impact event, because of the low matrix adhesion and mechanical properties of natural fibers, overall energy absorption is

low. However, research has shown that the inclusion of natural fibers into a neat resin has shown to improve impact toughness [36].

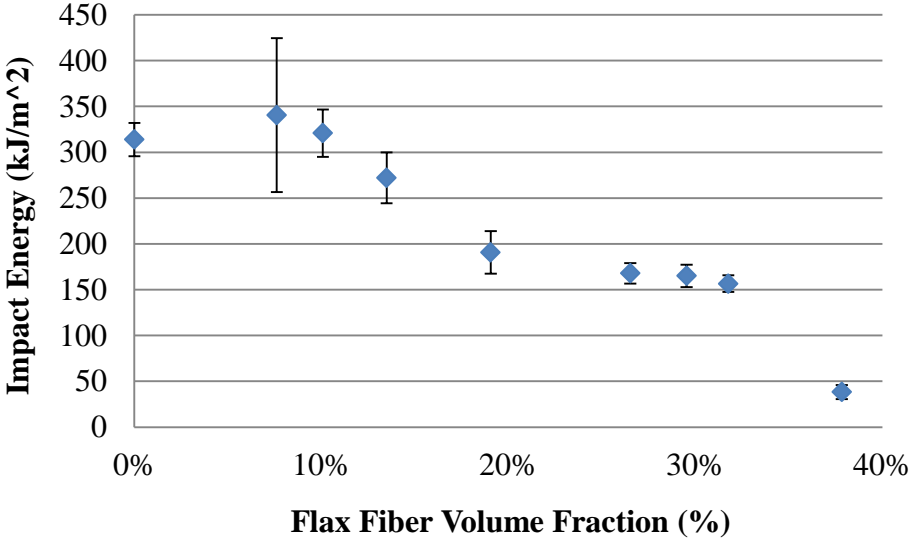


Figure 20. Impact energy versus flax fiber loading results from Charpy impact testing.

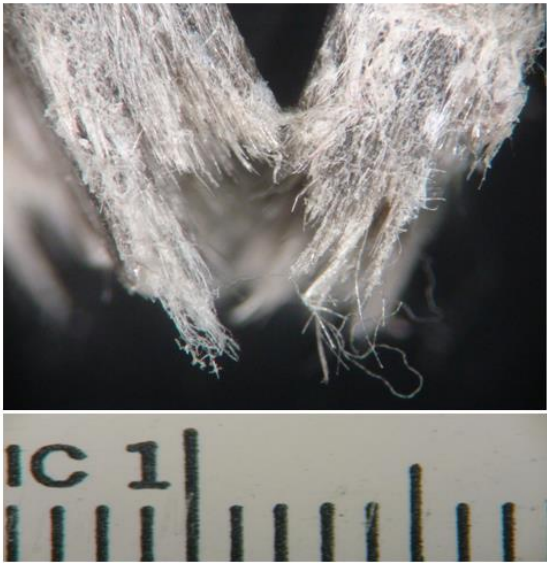


Figure 21. A plain flax fiber composite's side profile after an impact event (scale is in centimeters).

When discussing high impact performance, carbon fibers generally do not come to mind as a result that, generally speaking, high modulus fiber composites have generally been found to exhibit low impact strength [21]. However, when compared to natural fibers they display a much higher degree of impact performance. Looking at the obtained impact results, carbon fiber composites had an impact strength just above 300 kJ/m². Carbon fibers had several failure modes which were observed post impact event. Figure 22 shows that during an impact event, the composite failure modes occur which all help to dissipate impact energy and therefore increase impact strength. The two primary failure modes were fiber debonding and fiber breaking. As a result of the better matrix adhesion of carbon when compared to natural fibers, there is greater energy dissipation that occurs during a fiber debonding event. Similarly, as a result of carbon fiber's higher mechanical properties it takes more energy to break a carbon fiber than it does a flax fiber.

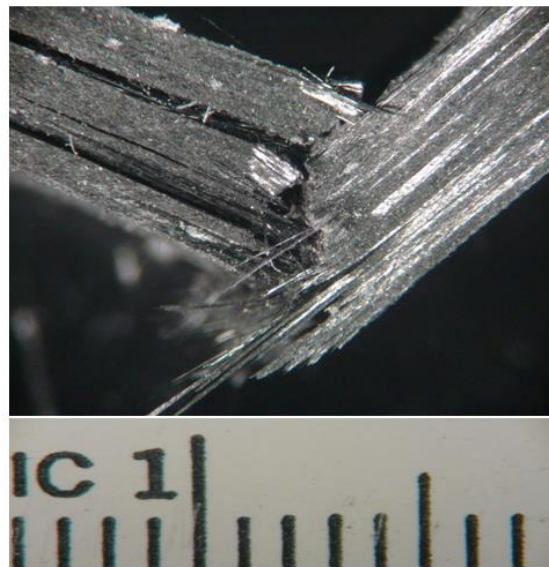


Figure 22. A plain carbon fiber composite's side profile after an impact event (scale is in centimeters).

It can be observed that specimen between 20 – 35% flax fiber volume fractions have close to similar impact strength. The explanation for this can be seen when examining the failure method. For the composites with high flax fiber volume fractions, the primary mode of failure is lamina debonding. Figure 23 shows the debonding of the flax fiber plies from themselves. However, the bonding between the flax fibers and the carbon fibers appears relatively stronger as debonding from the different fibers was not as common as debonding between flax fiber plies. One method that was not explored but could perhaps increase the impact strength between the flax fibers would be to incorporate a surface treatment to enhance the bonding between matrix and fiber which would increase the energy dissipation from a debonding event.

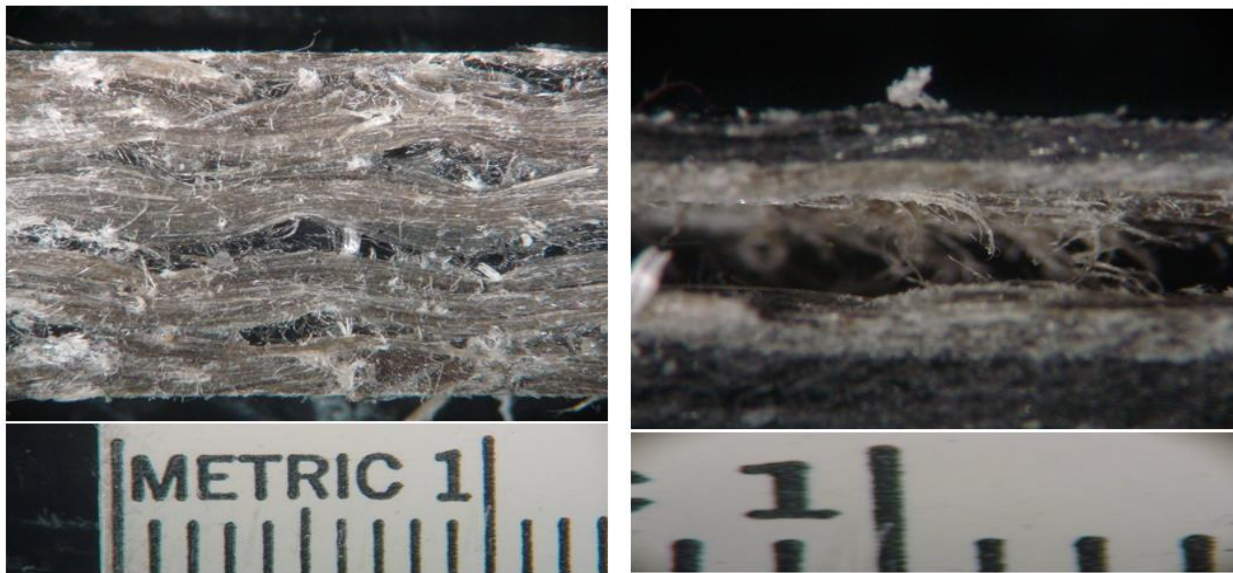


Figure 23. The debonding of the flax fiber ply from the carbon fiber ply (Vertical view (left) and horizontal view (right)) (scale is in centimeters).

Hybridized composites with less than 20% flax fiber volume fractions however, have increased impact strength than their greater than 20% flax fiber volume hybrid counterparts. The reason for this increase in impact strength can be seen in the mixture of failure modes that occur during impact. The failure modes that occurred were similar to the 20% flax fiber volume

fraction hybrid composites and the plain carbon composites. This combination of failure modes such as ply debonding and fiber breaking resulted in increased gains of impact strength which even surpassed those of plain carbon. An example of the mixed failure modes can be seen in Figure 24. The fact that the low flax fiber volume composites displayed higher impact values than the plain carbon fiber composites is not uncommon. Researchers have found that by incorporating small percentages of low-modulus but high strength fibers is an effective means of increasing the impact performance of composites [21].

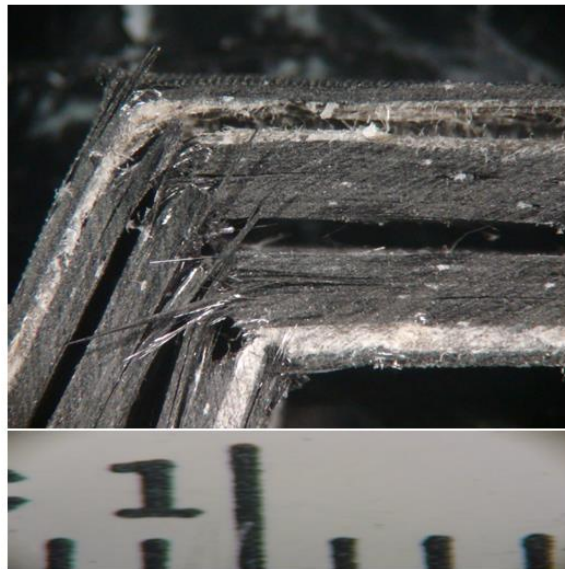


Figure 24. A low flax fiber volume fraction hybrid composite's side profile after an impact event (scale is in centimeters).

4.4. Tensile Testing Results

Tensile testing was performed on all the processed panels, and the chord modulus of elasticity results from the test can be seen below in Figure 25. It can be observed that with an increase in flax fiber content, there is also a proportionate decrease in chord modulus. This trend is to be expected as a result of the lower tensile stiffness of flax fibers.

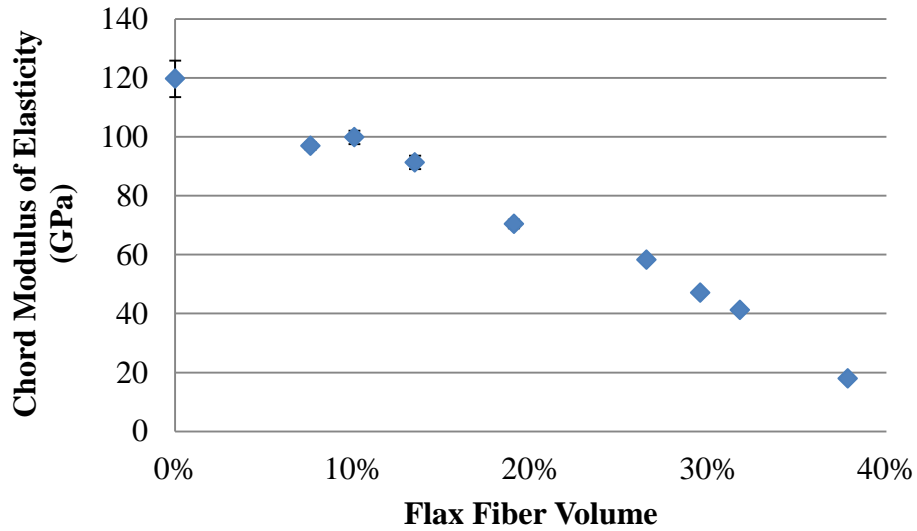


Figure 25. Chord modulus of elasticity versus flax fiber loading results.

When looking at how the stress is distributed throughout each ply in a hybrid composite during a tensile test, it can be noted that the carbon fibers are what drives the tensile properties as a result of their higher tensile modulus than flax fibers. Figure 26 shows what the stress distribution for flax and carbon hybrid composites would look like during a tensile test.

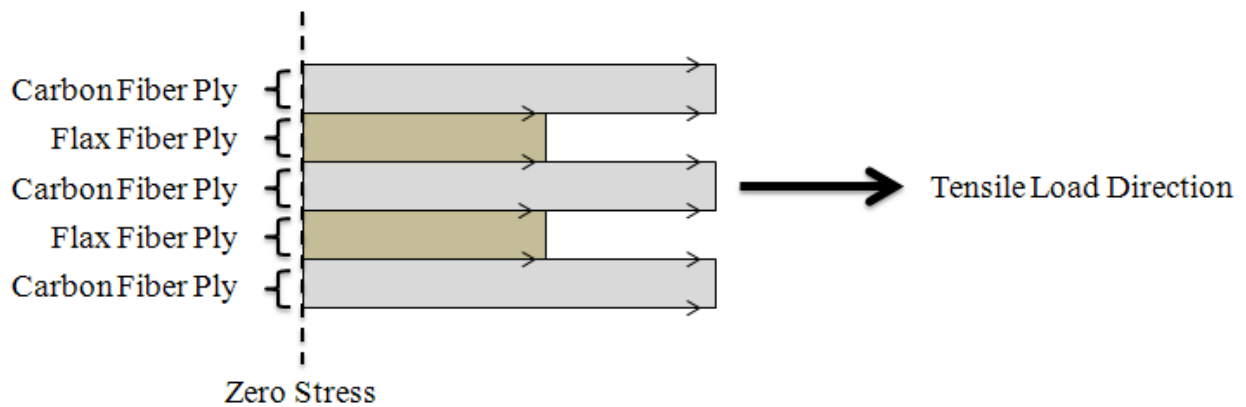


Figure 26. Tensile stress distribution in hybrid flax carbon composites.

The tensile strength results can be seen in Figure 27, where a similar trend as the chord modulus results can be observed. An increase in flax fiber content, results in a decrease in tensile strength. The primary mode of failure for hybrid composites during testing is a rupture of the outside carbon layers which would break and then debond themselves from the flax layers which would then trigger total catastrophic failure moments later. Ultimate strength results were only obtained for flax fiber volumes of 20% and greater. This was a result of tab failures which occurred when lower flax fiber volumes were substituted for increased carbon fiber volume content. Once composite tensile loads of approximately 11,000 lbf were reached tabs began to debond from the composite and composite failure was then unattainable.

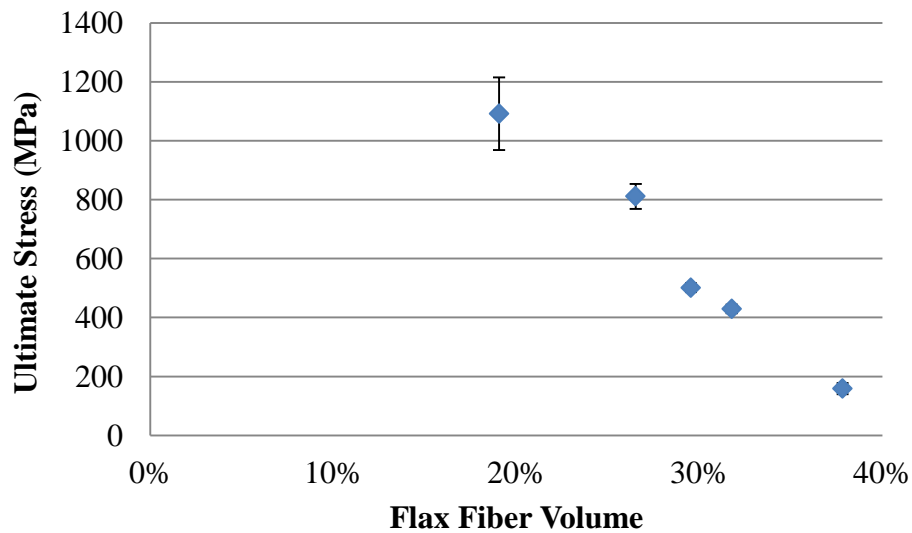


Figure 27. Ultimate stress versus flax fiber volume content test results.

4.4.1. Comparison of experimental results to theoretical results

Examining how the experimental values compared with those obtained theoretically, it was observed that the theoretical values were in good agreement. The figure below (Figure 28) shows the experimentally obtained data along with its theoretical modulus predictions. A simple

rule of mixtures approach was used to obtain the theoretical values. The difference in values ranges from 2-12% with plain flax having the highest deviation from theoretical values. An explanation for flax's higher deviation from theoretical values is that although it is classified as a unidirectional fabric, it is not purely unidirectional. Due to flax fiber processing, in order to produce a continuous fiber tow, fibers are wound together which causes the fibers to not be directly straight and inline.

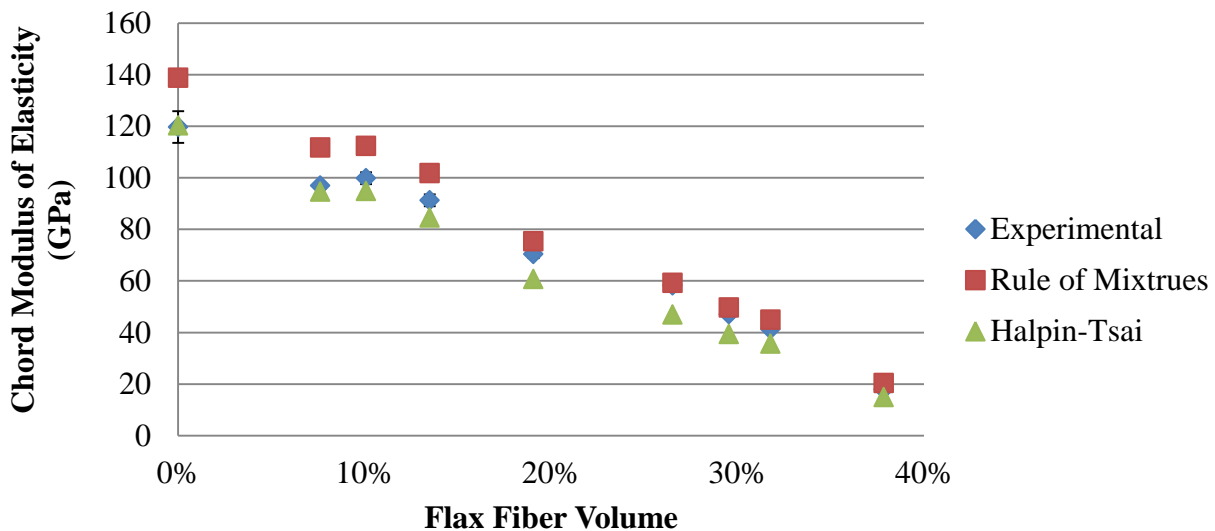


Figure 28. A comparison of the chord modulus of elasticity values obtained experimentally and theoretically.

The rule of mixtures method was initially called into question as a viable means of predicting tensile modulus in hybridized composites. Through experimentation, the rule of mixtures method was found to be an accurate means of modulus prediction for unidirectional laminate composites as a result of its low variance from experimental values. However, the Halpin-Tsai method was also used to compare experimental values to a theoretical model to determine if the model was a better predictor of hybridized composite modulus. Coefficient of

variance was used to determine which method was a better predictor of modulus. Figure 29 was developed to better understand the model's predictive characteristics. It can be observed that for low flax fiber volumes (<15%), the Halpin-Tsai model is a better predictor of modulus. This is because the Halpin-Tsai equation takes into account a fiber reinforcing coefficient which is calculated based on how well the fiber enhances the properties of a composite. This is determined from experimental values and how well the theoretical model compares to the experimental values. For the flax fibers used, the reinforcing efficiency is relatively low (22), while carbon fibers are almost ten times higher (202). So as higher volumes of flax fiber are introduced to the composite, the model begins to deviate from experimental values. The rule of mixtures model deviates at high values of both flax and carbon and begins to have improved variance at equal values of each fiber. This trend can be attributed to the assumptions that go into the models deviation such as continuous, parallel, and uniform cross-sectional fibers. Therefore, it can be understood that an average variance of 10% is to be expected.

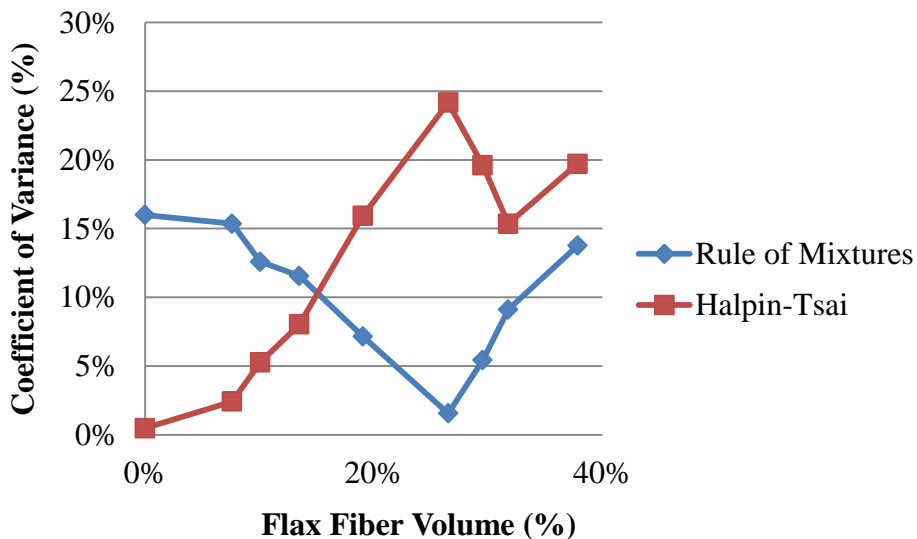


Figure 29. Coefficient of variance in different theoretical models versus flax fiber volume.

As previously discussed in the Background section, natural fibers have nonlinear elastic tensile behavior while synthetic fibers have linear elastic tensile behavior. When looking at the stress versus strain data for several performed tensile tests it can be observed that with an increase in carbon fiber content, there is an increase in linear elastic tensile behavior of the composite. The plotted stress versus strain curves can be seen in Figure 30. The degree of linear elastic tensile behavior was determined by fitting a linear trendline through the data points and evaluating the coefficient of determination. As the coefficient of determination approached unity, linear elastic tensile behavior was achieved while lower coefficients of determination equated to nonlinear elastic tensile behavior. An explanation for this increasing linearity with the incorporation of increasing amounts of carbon fiber is that carbon fiber is the dominate fiber in a hybrid composite during a tensile loading event. The incorporation of carbon fibers result in similar composite tensile behavior as to plain carbon fibers because its tensile properties are much higher than those of flax fibers.

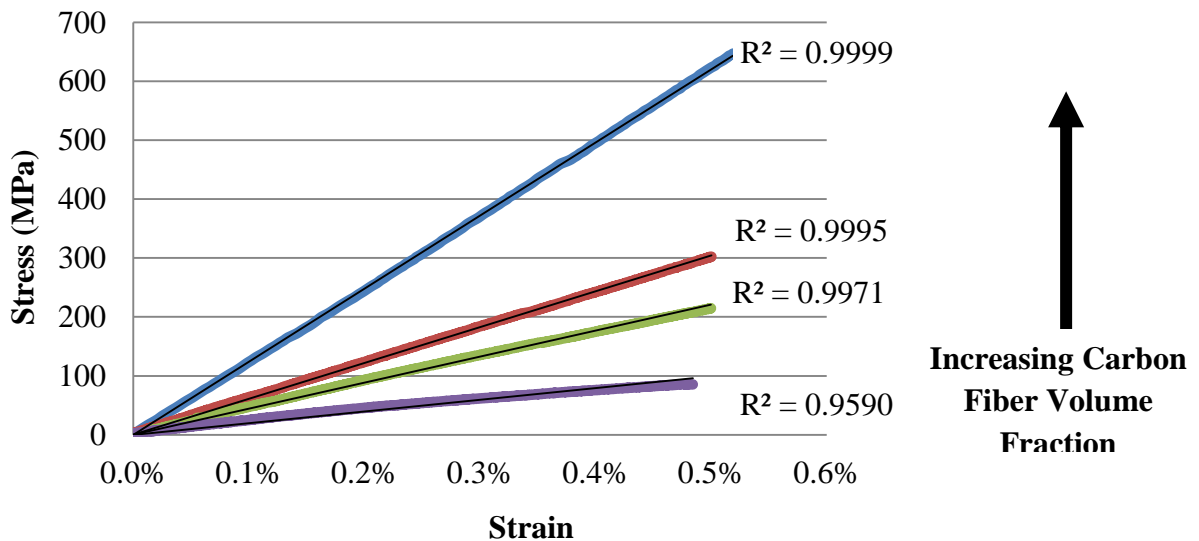


Figure 30. Linear and nonlinear elastic tensile behavior of composites determined through coefficient of determination values.

4.5. Vibration Testing Results

Vibration analysis was performed on the plain carbon fiber and flax fiber samples as well as the hybrid samples ranging 13-30% flax fiber volume fractions. The results from the single cantilevered beam vibration tests can be seen in Figure 31. The results showed that with an increase in alternate fiber loading there is an increase in composite damping ratio. An increase in damping ratio corresponds to an improvement in vibrational damping characteristics of a structure.

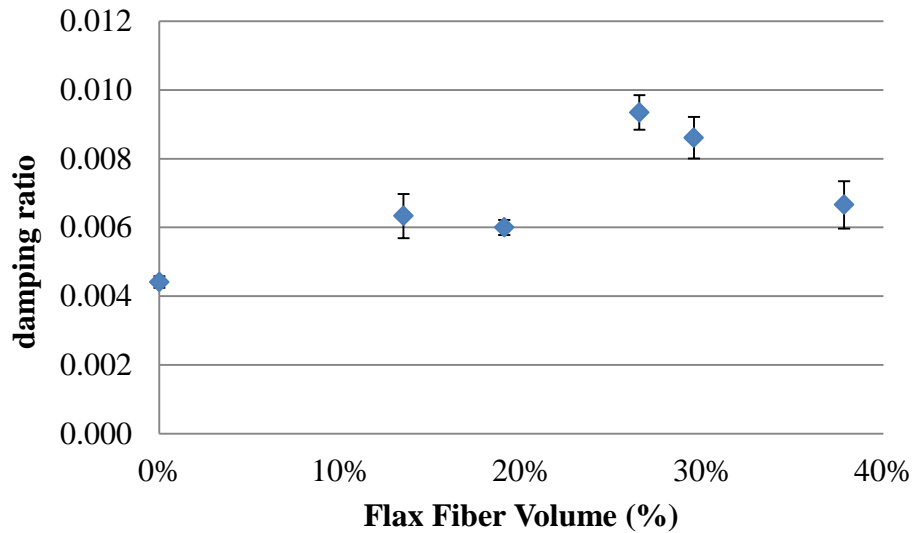


Figure 31. Damping ratios obtained from the single cantilever beam vibration test.

In order to get a better understanding of the obtained values it can be useful to compare the obtained damping ratios to damping ratios of different materials. When comparing the different damping ratios, it can be seen that composites offer improved damping characteristics. Figure 32 shows the damping ratios of different materials.

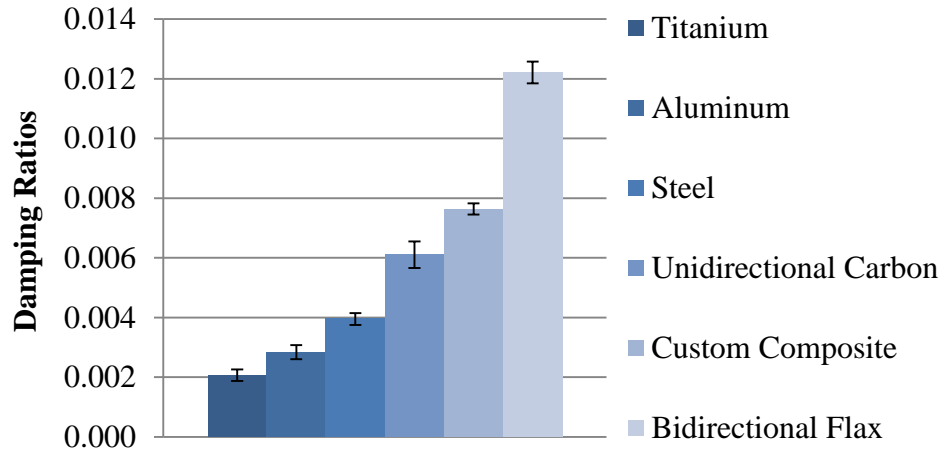


Figure 32. Damping ratios of different materials.

Looking at the results obtained in Figure 31, no distinct trend in damping ratio can be observed with an increase in alternate fiber loading, however, a clear gain in vibrational characteristics can be seen in the hybridized samples. Within the range of 10-20% flax fiber content, damping gains of around 40% were obtained over plain carbon fiber samples. While looking at the other end of the spectrum, within the range of 15-20% carbon fiber content, gains of around 35% were observed over plain flax fiber samples. Typical damping ratio values for structural composites have been found to be within 0.003 and 0.006 [37], which proves that the obtained damping ratios are reasonable. From literature it has also been found that hybridizing is a common method for improving damping characteristics in laminate composites [38].

The raw data from a single cantilever vibration test for a plain carbon and plain flax composite were overlaid on top of each other in Figure 33. From the results, it is clear that flax fibers have greater damping characteristics than carbon fibers. One explanation of this is that the flax fibers at the elementary fiber level can be thought of as a composite within a composite; the elementary fibers act as tiny shock absorbers in the composite and dissipate vibrational energy at

a local level before the vibrations have a chance to be transferred throughout the structure [17]. As a result of these tiny shock absorbers within the composite, overall improvements in composite damping can be seen with their incorporation.

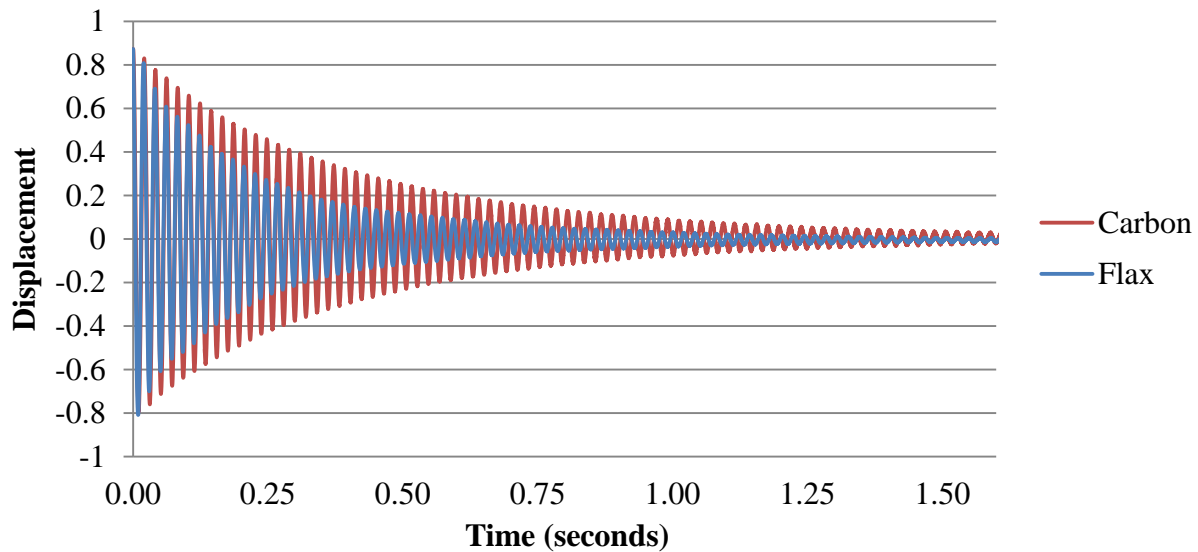


Figure 33. Raw data from a single cantilever test of plain carbon and plain flax composites.

4.6. Industrial Application

Composite materials have many different applications based on their generally high specific mechanical properties as well as their unique capability of being customized towards a specific application. However, sometimes the properties of a single fiber are incapable of meeting the demands of a specific application. Hybridized composites offer the opportunity to bridge the gap of shortcomings in a fiber by relying on a different fiber to provide the desired properties that are lacking in the original fiber.

One industry that is looking towards applying the concepts of hybridized composites to obtain a higher performing product is the agricultural industry. One area of application for

hybridized composites is in agricultural sprayer booms. An example of an agricultural sprayer boom can be seen in Figure 35. There are several advantages to switching to a hybrid composite sprayer boom over conventional materials as well as plain fiber composites. Through hybridizing, high strength and stiffness can be obtained in addition to achieving a lighter and cheaper material. The benefits of a lighter sprayer boom will reduce the ground compaction that occurs during the crop spraying process. High levels of ground compaction have been found to reduce crop production by making it difficult for roots to expand through the hard soil. A reduction in crop yield affects the achievable financial income of the end user. A lighter boom will also result in a decrease in fuel consumption. The incorporation of natural fibers has also been found to increase vibration damping. This will improve the fatigue properties of composites as well as a smoother ride for the tractor operator.



Figure 34. Agricultural sprayer boom.

A hybridized composite sprayer boom concept was developed for AGCO Corporation with the goal of developing a higher performance product. The concept of using a hybridized carbon and flax fiber composite was explored for the high mechanical properties the fibers

offered. The boom design structure concept can be viewed in Figure 35. The concept boom utilizes T-shaped cross-members (T-braces) that are adhesively bonded to the 4-frame. The cross-members were investigated for the potential of using the hybridized carbon/flax composite.

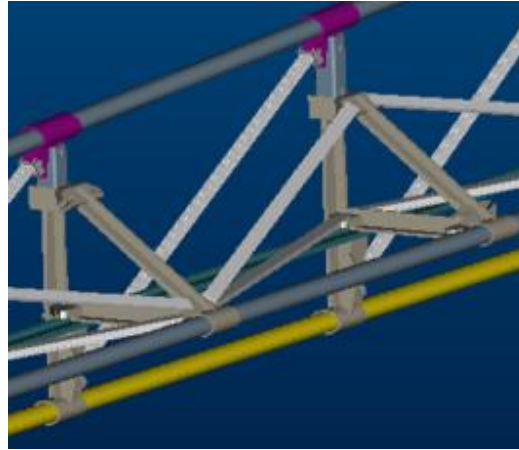


Figure 35. AGCO hybridized sprayer boom concept design.

The main objective of the AGCO project was to develop a composite that could replace the 6061 aluminum that is used for the cross-members. However, in order to be considered a successful replacement of 6061 aluminum, the developed composite must meet several prerequisites. The first requirement is that the hybridized composite possess a similar tensile stiffness to the aluminum. Tensile stiffness is defined as modulus of elasticity multiplied by the cross-sectional area of the material. In order to determine if this could be met, a preliminary study was conducted. The material properties used in the preliminary study can be viewed below in Table 4

Table 4. Material Properties Used in Preliminary Study

Material	Density (g/cm ³)	Young's Modulus (GPa)
6061 Aluminum	2.70	68.9
Carbon Fiber	1.80	227.5
Flax Fiber	1.50	0.5
Epoxy Resin	1.12	0.4

The study compared varying fiber volumes loadings of carbon fiber and flax fiber at a fixed total fiber volume fraction which ranged from 40%, 45%, and 50%. This meant that with an increase in flax fiber volume there was a proportional decrease in carbon fiber volume. A hybrid rule of mixtures approach was used to calculate the theoretical stiffness for the hybridized composite. Similar cross-sections were also used for simplicity. The results of the study can be seen below in Figure 36. It can be seen that everything above the red line (68.9 GPa-m) has a greater tensile stiffness than the 6061 aluminum. It can also be observed that the greater the total fiber volume fraction, the greater the range of allowable carbon and flax fiber volume combinations that provide an equal or greater tensile stiffness to 6061 aluminum.

The second requirement is that a weight saving be obtained. This was done by using the same procedure previously discussed. The results of the study can be viewed below in Figure 37. As a result of all the constituents in the hybridized composite possessing a lower density than aluminum, all allowable fiber loadings provide a lower density than 6061 aluminum.

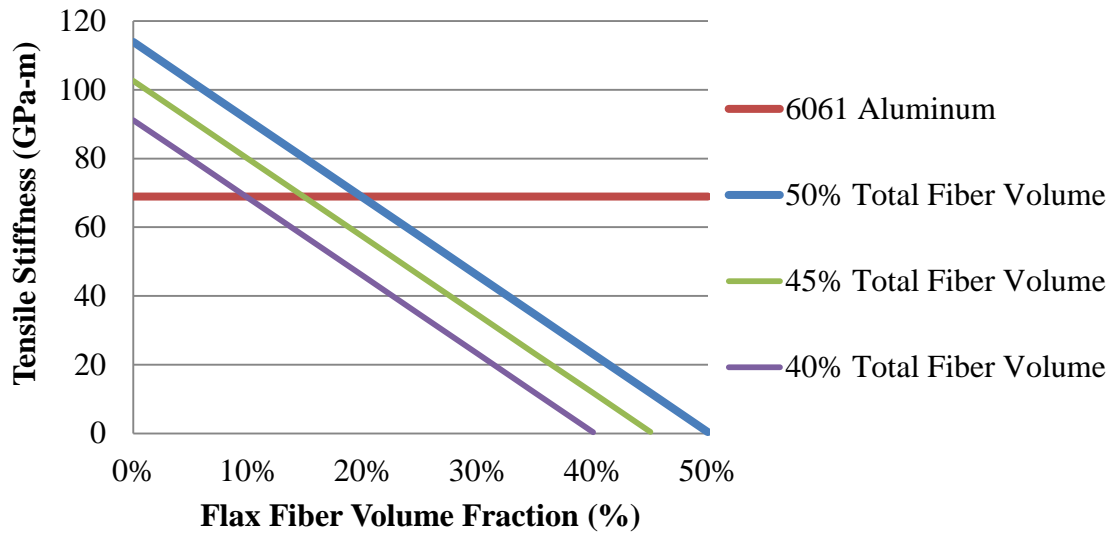


Figure 36. Preliminary study performed to determine fiber volume fractions necessary for obtaining a greater tensile stiffness than 6061 aluminum.

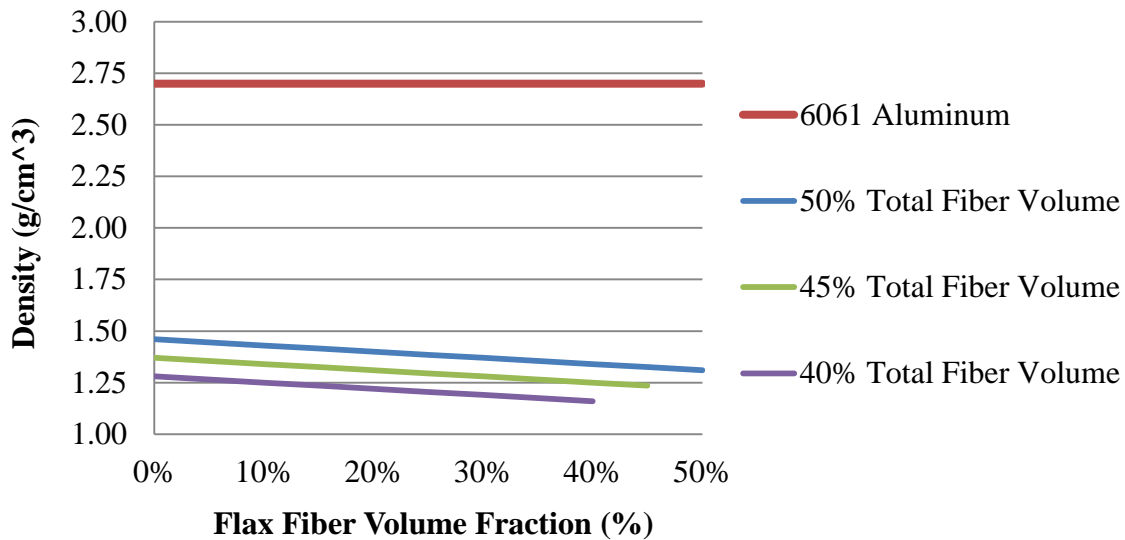


Figure 37. Preliminary study performed to determine fiber volume fractions necessary for obtaining a lower density than 6061 aluminum.

Once the analysis had been concluded, the design process was taken to the next step by an NDSU mechanical engineering senior design team. The team was tasked with developing a

prototype of the unit cell. The first step in validating the analysis was to develop a method for processing the composite T-braces. The T-braces were processed by using VARTM, which was used similarly to process the hybridized composite panels discussed previously in this paper. Instead of using caul plates, polypropylene (PP) polymer pre-forms were used to obtain the T-brace shape. The basic set-up for the T-bracing processing through VARTM can be seen in Figure 38. The infusion lines were placed at the base of the T-bar, while the vacuum line was placed on top of the pre-forms in order to force the resin to fight gravity to achieve better processing control of resin flow.

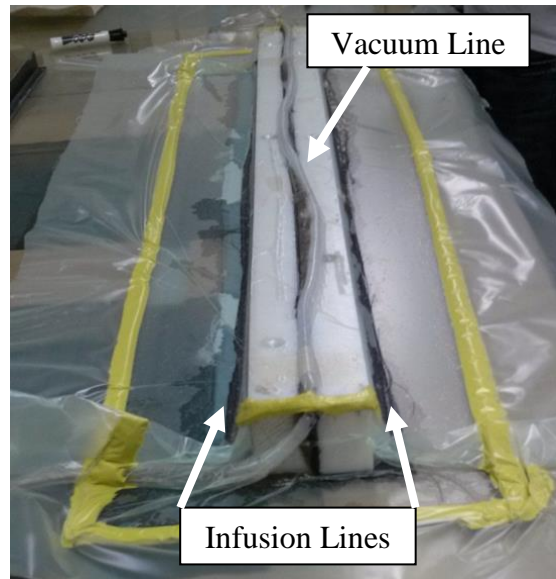


Figure 38. Processing T-shaped cross-members using VARTM.

Various stacking sequences were used to obtain optimum mechanical properties, although the general lay-up was similar to that used in processing the composites previously discussed. In addition, the carbon fiber ply orientations were all with the fibers going in the longitudinal direction of the T-brace while the hemp fiber was in a randomly oriented mat. The

basic configuration can be seen in Figure 39. Black represents carbon fiber and orange represents flax fibers.

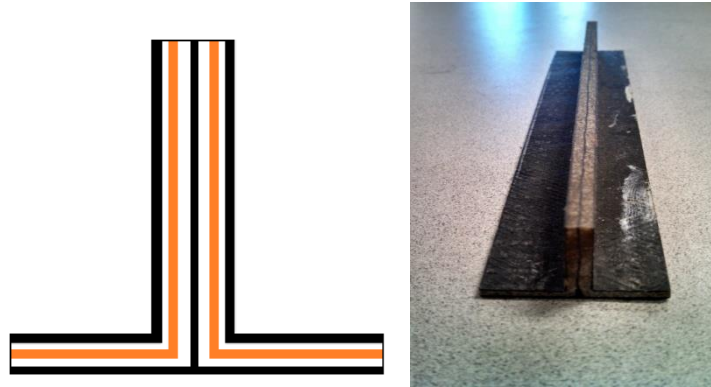


Figure 39. Fiber stacking sequence for T-shaped composite cross-members (left) and the finished product (right).

Using the AGCO sprayer boom design, two simplistic prototypes were created. The first prototype was made using aluminum T-braces while the other one uses the hybridized carbon and flax T-braces. The prototypes can be seen in Figure 40.

A plate was attached to the outside surface of the unit cell so that a hydraulic cylinder could apply a load to the unit cell and the deflection versus load could be measured. The tests showed that the composite T-braces showed a higher stiffness. However, the test was invalid because the unit cell mounts began to yield as the test progressed and higher loads were placed on the unit cell. Although for lower loadings the test could be considered accurate. The composite unit cell did however show a decrease in weight as a result of the composites lower density.

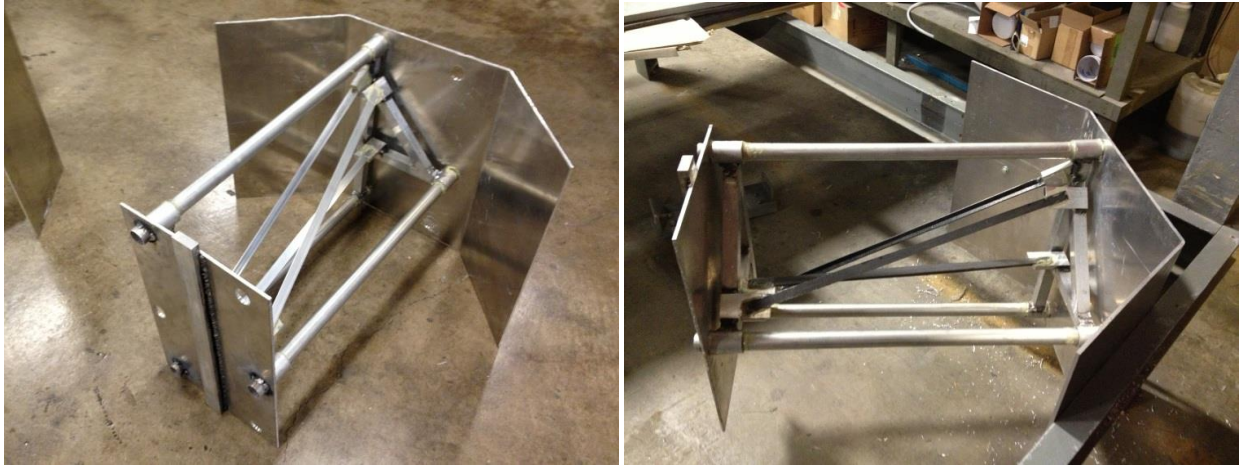


Figure 40. Finished AGCO prototype for the adhesively bonded unit cell. Unit cells using aluminum (left) and hybridized carbon and hemp (right) T-braces.

5. CONCLUSIONS AND FUTURE WORK

Hybridizing synthetic fibers with natural fibers has been found to be an effective method for improving the mechanical properties which have generally limited the full scale implementation of natural fibers composites into structural applications. When compared to 6061 aluminum, hybridized composites at a flax fiber volume fraction of 20% (which was determined to be of similar tensile stiffness in the preliminary study) were found to exhibit the following gains mechanical properties:

Tensile properties:

Chord Modulus: 2%

Tensile Strength: 252%

Vibrational properties:

Damping Ratio: 114%

In addition to the mechanical properties, there was also a 49% weight savings as a result of the reduced composite density.

In addition to the gains in mechanical properties which resulted from hybridizing synthetic fibers with natural fibers, it was also concluded that typical micromechanical modeling approaches such as rule of mixtures are a successful method for modulus prediction. It was determined that the rule of mixtures model has an on average a 10% over estimation from experimental results. The over estimation can stem from many of the assumptions that go into the model's deviation such as perfect bonding between fiber and matrix, parallel and continuous

fibers, and zero residual stresses. However, the model has shown to be a successful tool for hybridized fiber composites modulus prediction.

While the rule of mixtures model was successful at producing values that were within 10% on average of experimental values, the Halpin-Tsai model was capable of producing values of higher accuracy at flax fiber volume loadings of less than 15%. At flax fiber volume loadings greater than 15% however, the Halpin-Tsai model under predicted modulus values by as much as 15-25%. This was a result of carbon's higher fiber reinforcing efficiency value which was approximately ten times larger than flax's.

While the works covered in this paper provide a fairly comprehensive understanding of the effects on mechanical properties that occur with hybridizing flax and carbon fibers, there is still work that could be done to add to the knowledge base of hybridizing carbon and flax fibers. The next phase of testing should involve composites that have comingled fibers instead of fabric plies. This would remove the mechanical trends that arise from ply dependency. While the goal of this paper was to minimize these effects so that a clearer understanding of role that increases in flax fiber volume fraction played in mechanical trends could be observed, it would be unwise to say that they did not occur. One method of processing comingled hybridized fiber composites would be through a pultrusion process.

In order to achieve a better representation of actual mechanical data, another area to examine would be natural fiber surface treatments. Researchers have found improved mechanical properties with the incorporation of surface treatments which provide a higher degree of bonding between fiber and matrix. When looking at the failure modes of the hybrid impact specimen particularly, the main cause of failure was natural fiber debonding. This debonding could be

potentially reduced through a surface treatment, which intern would provide improved impact strengths. Through surface treatments, there could be improved mechanical properties across the board and a truer sense of what is occurring could be determined.

The end goal of this research is to provide a means for natural fibers to expand into structural applications. Before natural and synthetic hybrid fiber composites can be fully utilized in structural applications it is important to understand how they will perform in fatigue scenarios. Fatigue data would provide design engineers with the information necessary to use hybrid composites in suitable applications.

Another area that could help engineers better apply hybrid composites would be to investigate environmental effects on mechanical properties. This would include subjecting composites to a weathering chamber for a period of time then performing mechanical tests. This could range from water absorption, thermal aging, examination of how hybrids perform at various temperatures, etc.

REFERENCES

- [1] D. B. Dittenber and H. V. GangaRao, "Critical review of recent publications on use of natural composites in infrastructure," *Composites: Part A*, vol. 43, pp. 1419-1429, 2012.
- [2] H. Abdul Khalil, S. Hanida, C. Kang and N. Nik Fuaad, "Agro-hybrid composites: the effects on mechanical and physical properties of oil palm fiber (EFB)/glass hybrid reinforced polyester composites," *Journal of Reinforced Plastics and Composites*, vol. 26, pp. 203-218, 2007.
- [3] S. Mishra, A. Mohanty, L. Drzal, M. Misra, S. Parija, S. Nayak and S. Tripathy, "Studies on mechanical performance of biofibre/glass reinforced polyester hybrid composites," *Composites Science and Technology*, vol. 63, pp. 1377-1385, 2003.
- [4] K. Sabeel Ahmed and S. Vijayarangan, "Tensile, flexural and interlaminar shear properties of woven jute and jute-glass fabric reinforced polyester composites," *Journal of materials processing technology*, vol. 207, pp. 330-335, 2008.
- [5] K. John and V. S. Vaidu, "Effect of fiber content and fiber treatment on flexural properties of sisal fiber/glass fiber hybrid composites," *Reinforced Plastics and Composites*, vol. 23, pp. 1601-1605, 2004.
- [6] N. Venkateshwaran, A. Elayaperumal and G. K. Sathiya, "Prediction of tensile properties of hybrid-natural fiber composites," *Composites: Part B*, vol. 43, pp. 793-796, 2012.
- [7] J. Mirbagheri, M. Tajvidi, J. C. Hermanson and I. Ghasemi, "Tensile properties of wood flour/kenaf fiber polypropylene hybrid composites," *Journal of Applied Polymers Science*, vol. 105, pp. 3054-3059, 2007.
- [8] O. Faruk, A. K. Bledzki, H.-P. Fink and M. Sain, "Biocomposites reinforced with natural fibers: 200-2010," *Progress in Polymer Science*, vol. 37, pp. 1522-1596, 2012.
- [9] S. Joshi, L. Drzal, A. Mahanty and S. Arora, "Are natural fiber composites environmentally superior to glass reinforced composites?," *Composites: Part A*, vol. 35, pp. 371-376, 2004.
- [10] J. Holbery and D. Houston, "Natural-fiber-reinforced polymer composites in automotive applications," *JOM*, vol. 58, no. 11, pp. 80-86, 2006.

- [11] M. Jawaid and H. Abdul Khalil, "Cellulosic/synthetic fibre reinforced polymer hybrid composites: A review," *Carbohydrate Polymers*, vol. 86, pp. 1-18, 2011.
- [12] A. Bismarck, S. Mishra and T. Lampke, "Plant fibers as reinforcement for green composites," in *Natural fibers, biopolymers, and biocomposites*, Taylor & Francis, 2005, pp. 37-108.
- [13] L. Sherman, "Natural fibers: the new fashion in automotive plastics," *Plastic technology online*, 1999. [Online]. Available: www.ptonline.com. [Accessed 20 2 2013].
- [14] A. K. Mohanty, M. Misra and L. T. Drzal, "Surface modifications of natural fibers and performance of the resulting biocomposites: an overview," *Composite Interface*, vol. 8, pp. 313-343, 2001.
- [15] A. K. Mohanty, M. Misra and G. Hinrichsen, "Biofibres, biodegradable polymers and biocomposites: an overview," *Macromol Mater Eng*, vol. 276, pp. 1-24, 2000.
- [16] M. A. Fuqua, S. Huo and C. A. Ulven, "Natural fiber reinforced composites," *Polymer Reviews*, vol. 52, no. 3, pp. 1558-3724, 2012.
- [17] "Flaxcarbon," Museeuw Bikes, 2013. [Online]. Available: <http://en.museeuw.com/technology/flaxcarbon/flaxcarbon>. [Accessed 8 April 2013].
- [18] M. P. Staiger and N. Tucker, "Properties and performance of natural-fibre composites," in *Natural-fibre composites in structural applications*, Cambridge, Woodhead Publishing, 2008, pp. 269-300.
- [19] M. Joh and S. Thomas, "Biofibres and biocomposites," *Carbohydrate Polymers*, vol. 71, pp. 343-364, 2008.
- [20] A. K. Bledzki and J. Gassan, "Composites reinforced with cellulose based fibres," *Progress in Polymer Science*, vol. 24, pp. 221-274, 1999.
- [21] B. D. Agarwal, L. J. Broutman and K. Chandrashekhara, *Analysis and Performance of Fiber Composites*, New Jersey: John Wiley & Sons, Inc., 2006.
- [22] P. K. Mallick, *Fiber Reinforced Composites*, New York: CRC Press, 2008.

- [23] B. Z. Jang, *Advanced Polymer Composites*, Materials Park: ASM International, 1994.
- [24] D. Bender, J. Schuster and D. Heider, "Flow rate control during vacuum-assisted resin transfer molding (VARTM) processing," *Composites Science and Technology*, vol. 66, pp. 2265-2271, 2006.
- [25] B. W. Grimsley, P. Hubert, X. Song, R. J. Cano, A. C. Loos and B. R. Pipes, "Flow and compaction during the vacuum assisted resin transfer molding process," NASA, Hampton, 2001.
- [26] I. M. Daniel and O. Ishai, *Engineering Mechanics of Composite Materials*, new york: Oxford University Press, 2006.
- [27] C. T. Sun and R. S. Vaidya, "Prediction of composite properties from a representative volume element," *Composites Science and Technology*, vol. 56, pp. 171-179, 1996.
- [28] N. F. Dow, "Study of Stresses Near a Discontinuity in a Filament-Reinforced Composite Materials," General Electric Company report No. TIS R63 SD61, Barrington, 1963.
- [29] E. Mader and S. Zhandarov, "Characterization of fiber/matrix interface strength: applicability of different tests, approaches and parameters," *Composites Science and Technology*, vol. 65, pp. 149-160, 2005.
- [30] R. Mao and G. Sun, "A study of the interaction between matrix crack and matrix-fibre interface," *Engineering Fracture Mechanics*, vol. 51, no. 3, pp. 469-477, 1995.
- [31] C. C. Chamis, *Micromechanics Strength Theories*, New York: Academic, 1966.
- [32] J. C. Halpin and J. L. Kardos, "The Halpin-Tsai Equations: a Review," *Polymer Engineering & Science*, vol. 16, no. 5, p. 344-352, 1976.
- [33] Hexcel Corporation, [Online]. Available: <http://www.hexcel.com/Resources/DataSheets/Fabrics-Data-Sheets/GA130.pdf>. [Accessed 13 March 2013].
- [34] Composites Evolution Ltd., [Online]. Available: <http://compositesevolution.com/Portals/0/Biotex%20Flax%20Unidirectional%20TDS%200March%202012.pdf>. [Accessed 13 March 2013].

- [35] Huntsman Corporation, [Online]. Available: http://krayden.com/tds/hunts_aradur_8602_tds.pdf. [Accessed 13 March 2013].
- [36] H. N. Dhakal, Z. Y. Zhang, M. O. Richardson and O. A. Errajhi, "The low velocity impact response of non-woven hemp fibre reinforced unsaturated polyester composites," *Composite Structures*, vol. 81, pp. 559-567, 2007.
- [37] T. Irvine, "Damping properties of materials," 8 November 2004. [Online]. Available: <http://www.cs.wright.edu/~jlater/SDTCOutreachWebsite/damping%20properties%20of%20materials.pdf>. [Accessed 2 April 2013].
- [38] R. Chandra, S. Singh and K. Gupta, "Damping studies in fiber-reinforced composites - a review," *Composite Structures*, vol. 46, no. 1, pp. 41-51, 1999.